ChinaSpec: a Network for Long-term Ground-based Measurements of Solar-induced Fluorescence in China

Yongguang Zhang[1,2,3*], Qian Zhang[1], Liangyun Liu[4], Shaoqiang Wang[5], Yangjian Zhang[5], Weimin Ju[1,2], Jianwu Tang[6], Xudong Zhu[7], Guangsheng Zhou[8], Li Zhou[8], Feng Wang[9], Ying Huang[6], Jinsong Zhang[10], Xuguang Tang[11], Zaoying Zhang[1,2], Bo Qiu[1], Xiaokang Zhang[1,2], Songhan Wang[1,2], Changping Huang[4]

[1]International Institute for Earth System Sciences, Nanjing University, Nanjing, Jiangsu 210023, China.

[2]Jiangsu Provincial Key Laboratory of Geographic Information Technology, Key Laboratory for Land Satellite Remote Sensing Applications of Ministry of Natural Resources, School of Geography and Ocean Science, Nanjing University, Nanjing, Jiangsu 210023, China.

[3]Huangshan Park Ecosystem Observation and Research Station, Ministry of Education, China

[4]Aerospace Information Research Institute, Chinese Academy of Sciences, Beijing 100094, China

[5]Key Lab of Ecosystem Network Observation and Modelling, Institute of Geographic Sciences and Natural Resources Research, Chinese Academy of Sciences, Beijing 100101, China

[6]State Key Laboratory of Estuarine and Coastal Research, Institute of Eco-Chongming, East China Normal University, Shanghai 200241, China

[7]Key Laboratory of the Coastal and Wetland Ecosystems (Ministry of Education), College of the Environment and Ecology, Xiamen University, Xiamen, Fujian 361102, China

[8]State Key Laboratory of Severe Weather, Chinese Academy of Meteorological Science, Beijing 100081, China

[9]Institute of Desertification Studies, Chinese Academy of Forestry, Beijing 100091, China

[10]Key Laboratory of Tree Breeding and Cultivation of State Forestry Administration, Research Institute of Forestry, Chinese Academy of Forestry, Beijing 100091, China

[11]Chongqing Engineering Research Center for Remote Sensing Big Data Application, School of Geographical Sciences, Southwest University, Chongqing 400715, China

Corresponding author: Yongguang Zhang (yongguang_zhang@nju.edu.cn)

Key Points:

- ChinaSpec is a recently established network of ground-based Solar-induced Fluorescence (SIF) measurements.
- We present an introduction on the current status and challenges of ChinaSpec
- ChinaSpec now consists of 16 tower sites including 6 cropland sites, 4 grassland sites, 4 forest sites and 2 wetland sites.

Abstract

Remotely sensed solar-induced fluorescence (SIF) has emerged as a novel and powerful approach for terrestrial vegetation monitoring. Continuous measurements of SIF in synergy with concurrent eddy covariance (EC) flux measurements can provide a new opportunity to advance terrestrial ecosystem science. Here we introduce a network of ground-based continuous SIF observations at flux tower sites across the mainland China referred to as ChinaSpec. The network consists of sixteen tower sites until 2019 including 6 cropland sites, 4 grassland sites, 4 forest sites and 2 wetland sites. An automated SIF system was deployed at each of these sites to collect continuous high resolution spectra for high-frequency SIF retrievals in synergy with EC flux measurements. The goal of ChinaSpec is to provide long-term ground-based SIF measurements and promote the collaborations between optical remote sensing and EC flux observation communities in China. We present here the details of instrument specifications, data collection and processing procedures, data sharing and utilization protocols, and future plans. Furthermore, we show the examples how ground-based SIF observations can be used to track vegetation photosynthesis from diurnal to seasonal scales, and to assist in the validation of fluorescence models and satellite SIF products (e.g., from OCO-2 and TROPOMI) with the measurements from these sites since 2016. This network of SIF observations could improve our understanding of the controls on the biosphere-atmosphere carbon exchange and enable the improvement of carbon flux predictions. It will also help integrate ground-based SIF measurements with EC flux networks which will advance ecosystem and carbon cycle researches globally.

Keywords: Biosphere-atmosphere carbon exchange; ChinaSpec; Solar-induced chlorophyll fluorescence (SIF); Ground-based continuous measurements; Eddy covariance flux; Terrestrial photosynthesis

1 Introduction

To understand the impacts of climate change, it is essential to monitor the dynamics of ecosystem carbon and water fluxes and their response to environmental changes in a warming world. Eddy covariance (EC) flux measurements have been widely used to quantify carbon, water vapor, and energy exchange between biosphere and atmosphere and improve our understanding of variations in these fluxes (Baldocchi, 2008). The global EC network (FLUXNET), with more than 900 registered sites, has been running for more than 20 years since the1990s (Baldocchi, 2019). However, the footprint of EC measurements is generally less than 1 km^2, and the sites are unevenly distributed around the world with biased spatial coverage towards flat topography and uniform ecosystem types. The insufficient spatial coverage of networks of EC flux sites makes it difficult to estimate gross primary productivity (GPP) of terrestrial ecosystem accurately at large scales. Therefore, from the global perspective, it is necessary to upscale tower-based observations of EC flux at the ecosystem level to regional and global levels.

Remote sensing (RS) offers a unique way to parameterize explicit plant information across multiple spatial scales, and thus improves simulations of carbon fluxes of terrestrial ecosystems at regional to global scales (Hilker et al., 2008). RS techniques (e.g., MODIS sensor) have long been used for large-scale assessments of vegetation conditions, usually through the so-called vegetation indices (VIs) and other vegetation parameters derived from spectral measurements of surface reflectance (e.g., Huete et al., 2002). As a complement to reflectance-based VIs, solar-induced fluorescence (SIF) offers new possibilities to monitor vegetation function from space (Guanter et al., 2014). The recent technical advances have enabled the global SIF retrievals from satellites sensors. Remote sensing of SIF in recent years has been proven to be a novel indicator of photosynthesis or GPP. There is a growing number of space-borne missions with SIF retrievals that has opened up new possibilities to better monitor carbon flux and upscale EC flux data (Guanter et al., 2014; Frankenberg et al. 2011; Joiner et al., 2013; Köhler et al., 2015; Köhler et al., 2018; Sun et al., 2018; Du et al., 2018).

However, the fundamental scale mismatch in space and time remains a big challenge to upscale the EC flux data with satellite remote sensing data. Compared to high frequency EC flux sampling, most satellite remote sensing data usually have moderate spatial resolution but limited temporal resolution (e.g., 500 m and 16 days for MODIS). This sampling mismatch between remote sensing and flux measurements hinder the direct comparison between these two types of measurements. In this respect, ground-based spectral measurements offer a unique opportunity to bridge the measurement gap between satellites and EC flux towers because they can be conducted at an appropriate scale that more closely matches the spatial and temporal scales of the EC fluxes. Numerous studies have shown the advantages of ground-based measurements of spectroscopy to connect vegetation optical properties to flux measurements (e.g., Hilker et al., 2008; Balzarolo et al., 2011; Cogliati et al., 2015; Porcar-Castell et al., 2015; Aasen et al. 2019; Mohammed et al. 2019). The recent advances in sensor design and application have enabled the automated field optical sampling at the scale of flux tower footprints. With respect to the SIF measurements, a number of hyperspectral instruments has been deployed in the field since 2014 to support the rapid development of SIF retrievals from satellite missions (Cogliati et al., 2015; Yang et al., 2015; Yang et al., 2018a; Magney et al., 2019; Shan et al., 2019; Aasen et al. 2019; Zhang et al., 2019). This is benefited from the use of some commercially available spectrometers with high spectral resolution and signal-to-noise (SNR) ratio (e.g., QEPro from Ocean Optics,

Inc., Dunedin, FL, USA), which enable the direct retrievals of canopy SIF in the field. During the last few years, several novel ground-based SIF systems, including SFLUOR box (Cogliati et al., 2015), FluoSpec2 (Yang et al., 2018b), Photospec (Grossmann et al, 2018), FAME (Gu et al., 2019), FLOX (JB Hyperspectral Devices), SIFSpec (Du et al., 2019), Rotaprism (Josep A. Berry, personal communication), SIFPrism (Zhang et al., 2019), and Piccolo Doppio (MacArthur et al., 2014) have been developed and operated for autonomous continuous observations of canopy SIF in the field over years covering different vegetation types around the world. These SIF measurements are generally made together with EC flux observations providing opportunities for the integration between them and also for direct comparison and validation of satellite SIF data (Yang et al., 2015; Parazoo et al., 2019). Overall, ground-based spectral instruments could be used as a "bridge" between the EC flux and satellite remote sensing data. In addition, drone-based or airborne SIF measurements could be further address the issue of scale mismatch (MacArthur et al., 2014; Rascher et al., 2015; Frankenberg et al., 2018).

Within this context, it is necessary to build a network with coordinated field spectral measurements concurrently with EC flux observations. Similar to the EC FLUXNET community (https://fluxnet.fluxdata.org/), several regional or global optical measurements have been established. For example, SpecNet (http://specnet.info) was founded and has been operatinal since 2003 for the integration of optical sampling with EC flux measurements across flux sites (Gamon et al., 2006; Gamon et al., 2010). Although this network has stimulated an international collaboration between remote sensing and flux communities, the field sites are mainly located in North America (NA). Recently, the European remote sensing community has also started to establish its own optical network, EUROSPEC, to conduct long-term ground-based optical measurements at the representative EC towers in the European Union (EU) (Porcar-Castell et al., 2015; Aasen et al. 2019; Cendrero-Mateo et al. 2019; Pacheco-Labrador et al. 2019). EUROSPEC plays a fundamental role in supporting European satellite missions, such as the Fluorescence Explorer (FLEX). Overall, these networks mainly cover the geographical areas of EU and NA. Recently, the Chinese remote sensing and EC flux communities have also started to conduct ground-based spectral measurements.

In China, a network of collaborating sites and investigators has been founded starting in 2016 to conduct ground-based continuous optical measurements along with EC flux for ecosystem research. The network is referred to as ChinaSpec (http://chinaspec.nju.edu.cn). The goal of ChinaSpec is to promote the integration of optical measurements, especially the novel SIF measurements, with EC flux measurements for better understanding the controls of climate and environmental factors on the biosphere-atmosphere fluxes of carbon and water vapor in China. A primary goal of ChinaSpec is to collect the long-term continuous SIF measurements in the field over different vegetation types across the country, and to fill the gap between EC flux and satellite SIF observations.

The overall aim of this paper is to present an introduction on the current status and challenges of the ChinaSpec network. A primary ChinaSpec focus is on the ground-based SIF measurements at the flux sites within ChinaFLUX network (http://www.chinaflux.org/) (Yu et al., 2006; Yu et al., 2010), where the EC measurements have existed for more than ten years. Specifically, we emphasize on the current status of ChinaSpec and illustrate the usefulness of such network datasets for future research directions.

2 Instrumentation and data collection

2.1 Instrument description

Many SIF systems have been recently developed for ground-based observations (see reviews in Aasen et al., 2019). To have a high degree of consistency in instrumentation across the ChinaSpec network, two similar automated SIF systems are mainly used in ChinaSpec: Fluospec2 (Yang et al., 2018b) and SIFSpec (Du et al., 2019) (Figure 1a and Table 1) except for one site with FLOX. Though the controlling software is different in these systems, the core spectrometer, light path-switching approach and spectrum sampling strategy are the same. Both systems use purpose-built micro-computers to record data. The spectrometer used for SIF observation is QEPro or QE65Pro (OceanOptics, Inc., Dunedin, FL, USA). QEPro is an improved version of QE65Pro with high saturation threshold with digital number (DN) up to 200,000 (Max. DN of 65535 for QE65Pro). These two types of spectrometer are similar in spectral resolution and SNR, and both are suitable for SIF measurements. As spectrometer with only one input optical path, a "Y-shaped" splitter fiber-optic separating one optical path into two paths, and a fiber-optic shutter TTL or two inline TTL shutters (OceanOptics, Inc., Dunedin, FL, USA) switching between two input fibers are used to enable the spectrometers to nearly-simultaneously measure both solar irradiance and canopy radiance (Figure 1). One of the two input fibers is fixed upward for measuring the downwelling solar radiation equipped with cosine corrector CC-3 (OceanOptics, Inc., Dunedin, FL, USA), and another one is a bare fiber (OceanOptics, Inc., Dunedin, FL, USA) to collect the upwelling canopy radiation (Figure 1) with field of view (FOV) of 25°.

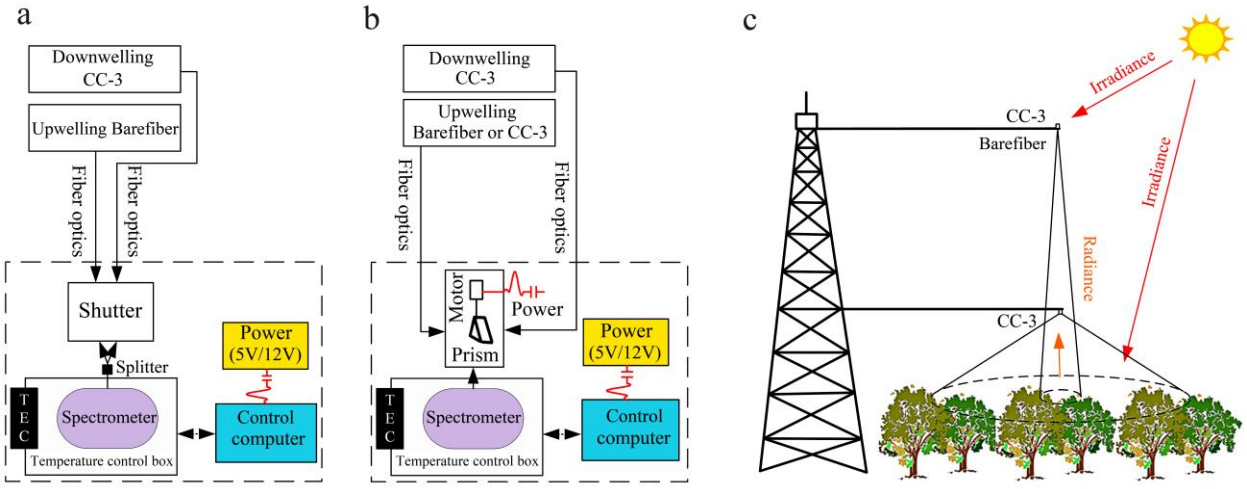

Figure 1. Schematic layout of the hyperspectral instrument used in ChinaSpec. (a) Fluospec2 or SIFspec system. (b) SIFprism system. (c) A drawing of field configurations for ground-based spectral measurements with upwelling bare fiber or cosine corrector CC-3.

The spectral range of these system is 650-800 nm (FWHM of ~0.3 nm) or 730-780 nm (FWHM of ~0.15 nm). Far-red SIF (760 nm) is measured at all the sites while red SIF (687) is only measured at some of these sites (Table 1). Recently, Zhang et al. (2019) compared the performances of these SIF systems (Fluospec2, SIFSpec, and FLOX) and found that they showed marginal differences in the diurnal patterns of SIF when measuring a homogeneous vegetation canopy. At several sites in ChinaSpec, another spectrometer HR2000+ (OceanOptics, Inc.,

Dunedin, FL, USA) with spectral range from 300 nm-1000 nm (FWHM of ~3 nm) is used to measure hyperspectral reflectance (see Table 1 for the sites). For these SIF systems, a temperature-controlled waterproof enclosure with external thermoelectric cooler is generally used for housing the spectrometer and keeping the environment temperature constant at around 25°C. This could ensure that the spectrometers work at a stable ambient temperature and stabilize the noise levels and radiometric response (Aasen et al., 2019).

2.2 Field instrumentation setups

Ground-based SIF measurement is complicated, and needs reliable field setups and measurement protocols (Aasen et al., 2019). In order to make reliable and comparable canopy SIF measurements in ChinaSpec, we adopt the recent design of automated SIF systems as in section 2.1 to allow a consistency in instrumentation across sites. Meanwhile, the same sampling strategy and instrument configurations are used to allow for inter-comparison between sites. In the ChinaSpec network, the SIF systems used (Fluospec2, SIFSpec, and FLOX) are all using hemispherical-conical (with conical upwelling sensor) configurations for SIF measurements at all sites (Table 1). These generally use bare fibers with FOV of 25° for upwelling measurements. In ChinaSpec, the view zenith angle of the upwelling sensor is currently installed as nadir or slightly off-nadir (< 10°) to constrain the effects of sun-viewer geometry variability. This uniform instrumentation setup could minimize the effects of viewing geometry across sites.

To integrate with EC flux measurements, proper instrumentation setups and protocols are needed to gain reliable and comparable SIF measurements. In ChinaSpec, the SIF systems are typically installed on the top of flux towers or close to flux towers (Figure 2). For tall canopy like forest, the systems are mounted on the platforms of tower as high as possible to gain a large FOV, and could see a large part of canopy to avoid only seeing 1-2 trees. At these sites, we suggest that the bare fiber can point slightly off nadir to avoid viewing any possible background close to the tower. Since the towers are typically high and large, it is recommended that the fiber optics should point to the south to avoid the influence of the shadow of the tower in other directions. The ends of fiber optics, where the solar and canopy radiation penetrate into the system, are better if they are far off the platform to avoid interfering the optical signal into the fiber. Therefore, the fiber optics should be extended along with horizontal-setup pipe (or equivalent devices, such as sectional bar) about 2-4 m away from the edge of the platform. We recommend that the systems are installed at least 10 m above the canopy (> 4 m in diameter of footprint) to view more trees. For short canopy (e.g., crop and grassland), a simple tripod with bracket can be used to hold the fiber optics steady (e.g., XLHT in Figure 2). The place should be within the footprint of the EC flux measurements. The measurement height is suggested at least 2 m above the canopy (> 1 m in diameter of footprint). Considering the homogeneity in these ecosystems at the EC sites, it is assumed that the covering area by bare fiber represents the canopy as covered by EC flux footprint.

When installing the SIF systems in the field, the downwelling fiber optics with CC-3 are vertically (upward) mounted on a horizontal metal plate installation device fixed on the pipe. The upwelling bare fibers are mounted on a horizontal metal plate which is fixed nadir or slightly off-nadir at the end of the pipe. It is suggested that the irradiance (downwelling) and radiance (upwelling) channels are installed at the same height. The fiber optics should be also tightly fixed to avoid any disturbances or movements. Furthermore, the cosine diffuser (CC-3) is suggested to keep dust, insects, and birds away and a periodical check is recommended for possible

degradation (Aasen et al., 2019). Additionally, a thermometer screen or similar instrument shelter could be used to cover the enclosure of the systems against precipitation and direct heat radiation (Figure 2).

To maximize the footprint matching with EC measurements, bi-hemispherical measurements with a fore optic diffuser are also conducted to capture both downwelling and upwelling irradiance since 2019 at one site of Jurong. A newly developed system called SIFprism (Zhang et al., 2019), which is similar to Rotaprism (Joseph Berry, personal communication), was installed to conduct bi-hemispherical measurements (Figure 1b and Table 1). A rotary prism, which is rotated by an electric motor inside a sealed and adiactinic box, is used to collect both downwelling and upwelling irradiance sequentially. SIFprism collects the spectrum with less integration time than that of Fluespec2 and SIFSpec (Zhang et al., 2019), which allows for fast collection of upwelling and downwelling irradiance. With bi-hemispherical configuration (Figure 1c), SIFprism can capture a larger field of the canopy even with lower height than hemispherical-conical measurements (Figure 1C). This is more relevant to the footprint of EC flux measurements (Gu et al., 2018). SIFprism has been tested in parallel with Fluospec2 since June in 2019 at a paddy-rice site of Jurong (Table 1). This comparison will provide a chance to investigate the pros and cons of different configurations for ground-based SIF observations, especially in synergy with EC flux measurements.

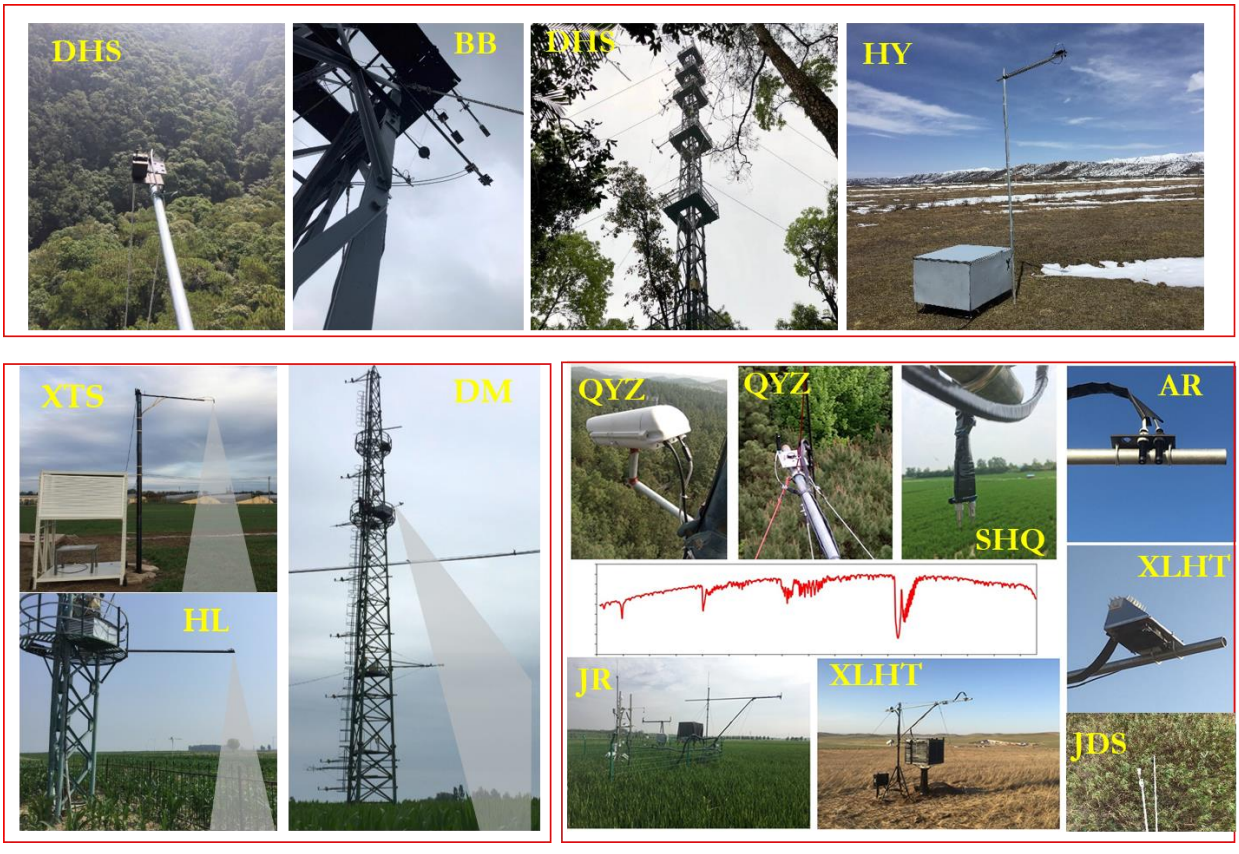

Figure 2. Examples of field set-up at several sites in ChinaSpec. The abbreviation of each site is referenced in Table 1.

2.3 Data collection and processing

All systems can automatically operate and collect spectral data under various field conditions. Solar irradiance (*E*) and canopy radiance/irradiance (*L*) are sequentially acquired, or a sandwich-method (*E*-*L*-*E*), which is helpful for evaluating if changes in illumination suitable for SIF observation during this short period, is used to measure spectral data (Cogliati et al., 2015; Aasen et al. 2019; Zhang et al., 2019). Dark current (DC) is simultaneously recorded after each spectral measurement for DC correction. Integration time (IT) of spectral measurement is automatically optimized to get as high and unsaturated values as possible to improve the SNR ratio:

$$IT = IT_{ini} \times targetDN / maxDN \tag{1}$$

where IT_{ini} is user-defined initial *IT*; *targetDN* is set about 60%-80% of the saturation DN value of spectrometer; and *maxDN* is the maximum value of a spectrum acquired with IT_{ini} at the beginning of each measurement.

Spectral data is recorded as DN values, which need to be radiometrically calibrated. Pre-mounted laboratory calibration using a tungsten halogen light source (HL -2000-CAL, Ocean Optics, USA) is conducted to calibrate hemispherical sensor (CC-3) and an integrating sphere to calibrate conical sensor (bare fiber) (Cogliati et al., 2015; Aasen et al. 2019; Pacheco-Labrador et al. 2019). In the field, regular cross radiometric calibration is generally performed using a light source (HL-2000-CAL, Ocean Optics Inc., USA) to calibrate CC-3 (up-looking channel), and a well-calibrated spectrometer with a standard reference panel (Spectralon, Labsphere, NH, USA) to calibrate bare fiber (down-looking channel) under a clear sky day around noon (Cogliati et al., 2015). The conversion of DN to radiance or irradiance can be finally expressed as (taking radiance as an example):

$$Radiance(\lambda) = \frac{L(\lambda) \times \left(DN_{obs}(\lambda) - DC_{obs}(\lambda)\right) \times IT_{cal}}{\left(DN_{cal}(\lambda) - DC_{cal}(\lambda)\right) \times IT_{obs}} \tag{2}$$

where λ represents the wavelength, Radiance (λ) is measured radiance by spectrometer, and *L* (λ) is the radiance of standard light resource. The subscript *obs* represents the field observation data recorded by the spectrometer and *cal* represents the calibration data. Both *DN* and *DC* are normalized by the IT used in each measurement to one second. Since the temporal stability of the calibrations are essential for long-term field SIF measurements, we recommend a regular in-field calibration (around every 3 months) in addition to a radiometric calibration in the lab before installation. At least one calibration should be conducted before the growing season.

Data quality control is operated before SIF retrieval following the protocol presented by (Cogliati et al., 2015) to exclude abnormal data caused by changing illumination conditions and other unpredictable reasons. At the present, we propose that the approaches used for SIF retrieval are Spectral Fitting Methods (SFM, Meroni & Colombo, 2006) and three-band Fraunhofer Line Depth (3FLD, Maier et al., 2003) in ChinaSpec. The 3FLD algorithm stems from the FLD principle, which requires spectral measurements at two bands, one inside and one outside a Fraunhofer line (Theisen, 2002). The FLD method assumes that reflectance and SIF maintain constant at the two bands. However, in fact, the two variables are far from being constant, especially for reflectance at 687 nm and SIF at 760 nm. Therefore, the FLD assumption has been questioned by several authors (Meroni & Colombo, 2006; Alonso et al., 2008; Gómez-Chova et

al., 2006; Meroni et al., 2009; Moya et al., 2006). The 3FLD method is based on an advanced assumption compared with FLD, namely reflectance and SIF vary linearly in the spectral domain considered, which overcomes the limitations given by FLD assumptions (Meroni et al., 2009; Cendrero-Mateo et al. 2019). The 3FLD-based SIF at 760 nm can been derived as:

$$SIF_{760} = \frac{\left(E_{left} \times w_{left} + E_{right} \times w_{right}\right) \times L_{760} - \left(L_{left} \times w_{left} + L_{right} \times E_{right}\right) \times E_{760}}{\left(E_{left} \times w_{left} + E_{right} \times w_{right}\right) - E_{760}} \quad (3)$$

where w_{left} and w_{right} denote the weight of the band, which is proportion to the length between the right/left band and the inner band. The subscripts "left" and "right" represent the band at the left and the right side of the absorption domain.

Differently, SFM employs two mathematical functions to describe r and SIF, which relaxes the assumptions of some FLD-based methods (Meroni et al., 2009; Cendrero-Mateo et al. 2019). Here, we use two linear functions to determine r and SIF in a restricted spectral domain around the O_2 absorption bands. Therefore, L(λ) can be expressed as:

$$\mathrm{L}(\lambda) = \frac{r_{mod}(\lambda)E(\lambda)}{\pi} + SIF_{mod}(\lambda) + \varepsilon(\lambda) \quad (4)$$

where $r_{mod}(\lambda)$ and $SIF_{mod}(\lambda)$ are linear functions describing r and SIF, respectively. $\varepsilon(\lambda)$ represents the error between the simulated and observed L(λ). With a large number of spectrum observations with high resolution less than 0.3 nm pledged by spectrometers and continuous measurements, the Eq. (4) can been overdetermined. Least square method is applied to solve the parameters (i.e. the respective gain and offset of $r_{mod}(\lambda)$ and $SIF_{mod}(\lambda)$) in the two functions. Then, SIF at 760 nm can been determined as $SIF_{mod}(760)$.

3 Current status of ChinaSpec

3.1 Current SIF Field sites in ChinaSpec

Sixteen sites have registered with ChinaSpec network, including 6 cropland, 4 grassland, 4 forest and 2 wetland sites across from subtropical to cold temperate zones and also covered from humid to semiarid regions (Figure 3 and Table 1). Locations of these sites are shown in Figure 3, and detailed information of each site can be found in Table 1. The spectral range of all these devices covers the range for far-red SIF (760 nm) and some of them cover both red SIF (687 nm) and far-red SIF (Table 1). Details on climate, soil and vegetation can be found in the ChinaSpec website. Here, we briefly present some basic information for these sites.

The cropland sites are distributed on the Zhangye oasis in northwest China (DM), the North China Plain (SQ), the Yangtze Plain (JR), the Northeast Plain (PJ) and North China Plain (HL and XTS) that monitor maize, rice and winter wheat. Among these cropland sites, HL, PJ and DM have only one growing season in a year with a maize or rice crop in the summer, while the other three have a rotation of two crops every year. Among the four forest sites, DHS is an evergreen broadleaf forest and QYZ is an evergreen needle forest. Both sites are located in a sub-tropical area with abundant rainfall and solar radiation. The BB site consists of managed pure *Osmanthus fragrans* stand (Yang et al., 2009). The XLD site is located in Jiyuan county, Henan province (410 m asl), and is dominated by cork oak (*Quercus variabilis blume*). The area of the

32-yr mixed plantation is approximately 7210 ha, with a stand density of 1905 trees ha^{-1} (Tong et al., 2019).

The four grassland sites include two alpine meadow (HY and AR), one semi-arid grassland (XLHT), and one sparse forest grassland (ZLQ). HY is located in an alpine meadow of the eastern Qinghai-Tibetan Plateau (3500 m asl) (Quan et al., 2019). The XLHT site (1250 m asl) is located in the Xilin River Basin, Inner Mongolia. This site has been fenced since 1999 and no grazing or other disturbance occurred thereafter (Zhang et al., 2016). Vegetation in this site is a typical steppe and dominated by perennial grasses (*Leymus chinensis* and *Stipa grandis*). The ZLQ site is Elm Sparse Forest Grassland Ecosystem (1300 m asl), and is located in the north-east of Otingdag Sandland, Inner Mongolia. The typical vegetation is natural sparse elm (*Ulmus pumila*) forest, shrubs and grass (Wang et al., 2019). The AR site is located in the Heihe River Basin (3000 m asl) with a typical temperate continental climate. The dominant vegetation is alpine meadow. In addition, two wetland sites (JDS-S and YX) are also included in ChinaSpec, which are very unique ecosystems for SIF measurements. JDS-S is a coastal salt marsh site located in the Jiuduansha Shoal of the Yangtze estuary to the East China Sea. It is dominated by *Spartina alterniflora* with 2 m height during the growing season. The YX site is located in the area of the Zhanjiang estuary to the South China Sea. It is a subtropical intertidal wetland vegetated with mangrove forests. The biggest challenge of observation for these two sites is the protection of the observation systems from humid and salty air to avoid corrosion of metal components.

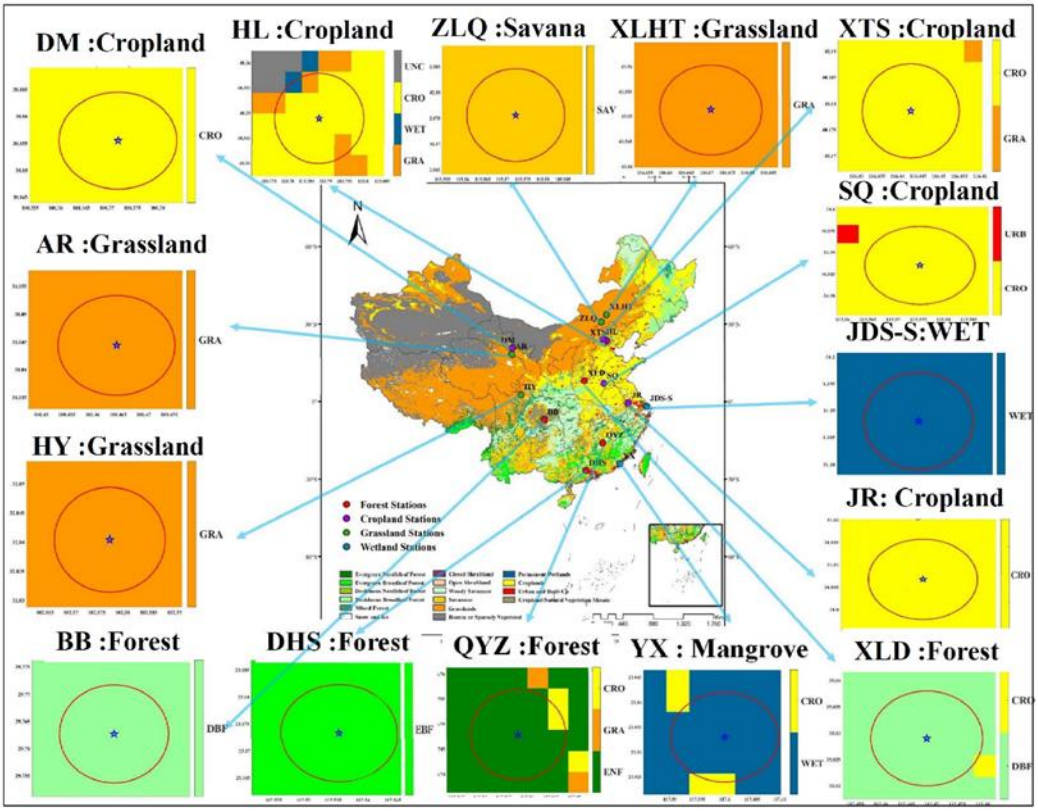

Figure 3. Summary of current field SIF sites in the network of ChinaSpec. Site names are defined in Table 1. The subplots are the vegetation type at each site (blue star). The base map is land cover map based on the MODIS Land Cover Type product (MCD12C1) at 500 m.

344 **Table 1.** Information of the field sites in ChinaSpec.

ID	Site Name	Site ID	Location	Coordinate	Height (m)*	Footprint (m^2)	PFT	Instrument	Spectral range & resolution**	Time Period
1	XiaoTang Shan	XTS	Beijing	40.1786 N 116.4432 E	4 /2.6	2.47/1.04	Cropland (winter wheat and maize rotation)	SIFSpec with QE65Pro	650- 800 nm, 0.3 nm	06/2017-
2	HuaiLai	HL	Hebei Province	40.3489 N 115.7882 E	2.5	0.95	Cropland (maize)	SIFSpec with QE65Pro	650- 800 nm, 0.3 nm	0-/2017-
3	DaMan	DM	Gansu Province	38.8555 N 100.3722 E	23	81.68	Cropland (maize)	SIFSpec with QE65Pro	650- 800 nm, 0.3 nm	05/2017-
4	ShangQiu	SHQ	Henan Province	34.5870 N 115.5753 E	12 /10	22.23/15.44	Cropland (winter wheat and maize rotation)	FluoSpec2 with QEPro and HR 2000+[#]	730-780 nm, 0.15 nm	07/2017-
5	JuRong	JR	Jiangsu Province	31.8068 N 119.2173 E	8	9.88	Cropland (rice and winter wheat)	FluoSpec2 with QEPro and HR 2000+[#]	730-780 nm, 0.15 nm	07/2016-
6	QianYan Zhou	QYZ	Jiangxi Province	26.7478 N 115.0581 E	15	34.74	Evergreen coniferous forest	FLOX with QEPro	650- 800 nm, 0.3 nm	03-12 /2017
7	XiLinhot	XLHT	Inner Mongolia	43.5513 N 116.6710 E	2.5	0.95	Grassland	FluoSpec2 with QEPro and HR 2000+[#]	730-780 nm, 0.15 nm	06/2017-
8	DingHuShan	DHS	Guangdong Province	23.1733 N 112.5361 E	18	50.03	Evergreen broadleaf forest	SIFSpec with QEPro	650- 800 nm, 0.3 nm	08/2017-
9	HongYuan	HY	Sichuan Province	32.8404 N 102.5775 E	3	1.39	Alpine meadow	SIFSpec with QEPro	650- 800 nm, 0.3 nm	04-07/ 2018
10	A'Rou	AR	Qinghai Province	38.0444 N 100.4647 E	25	96.50	Alpine meadow	SIFSpec with QE65Pro	650- 800 nm, 0.3 nm	04/2019-
11	YunXiao	YX	Fujian Province	23.9240 N 117.4147 E	7	7.57	Mangrove	FluoSpec2 with QEPro and HR 2000+#	730-780 nm, 0.15 nm	01/2018-
12	BeiBei	BB	Chongqing	29.7627N 106.3191E,	10	15.44	Managed Forest (Osmanthus)	SIFSpec with QEPro	650- 800 nm, 0.3 nm	9/2018-
13	ZhengLanQi	ZLQ	Inner Mongolia	42.9656N 115.9589E	2	0.62	Sparse forest grassland	FluoSpec2 with QEPro	730-780nm, 0.15 nm	6/2019-
14	XiaoLangDi	XLD	Henan Province	35.029 N 112.469 E	20	61.76	Deciduous broadleaf forest(oriental oak)	SIFSpec with QEPro	650- 800 nm, 0.3 nm	6/2019-
15	Jiuduansha-S	JDS-S	Shanghai	31.1881N 121.9489E	2	0.62	Coastal wetland *(Spartina)*	SIFSpec with QEPro	650- 800 nm, 0.3 nm	3/2019-
16	PanJin	PJ	Liaoning Province	40.8004 N, 122.0277 E	2.5	0.95	Cropland (rice)	FluoSpec2 with QEPro	650- 800 nm, 0.3 nm	5/2020-

345 *** Height above the canopy; ** Spectral resolution of spectrometer (FWHM); # HR2000+ is used to reflectance measurements within the range of 400 – 1000 nm.**

3.2 Data policy

ChinaSpec collaborates with the network of ChinaFLUX and other communities, and shares ground-based spectral and SIF data acquired from the sites of the network. The intent of sharing this dataset is to provide ground-based continuous SIF and reflectance measurements across multiple ecosystems in China to the broad community of scientists. The website (Figure 4, http://chinaspec.nju.edu.cn) is the platform for releasing the related information and sharing datasets of the sites registered in the ChinaSpec network since 2016 when the first dataset was collected. A few sites could also share EC flux data, but most sites are shared through ChinaFLUX network (Yu et al., 2006; Yu et al., 2010).

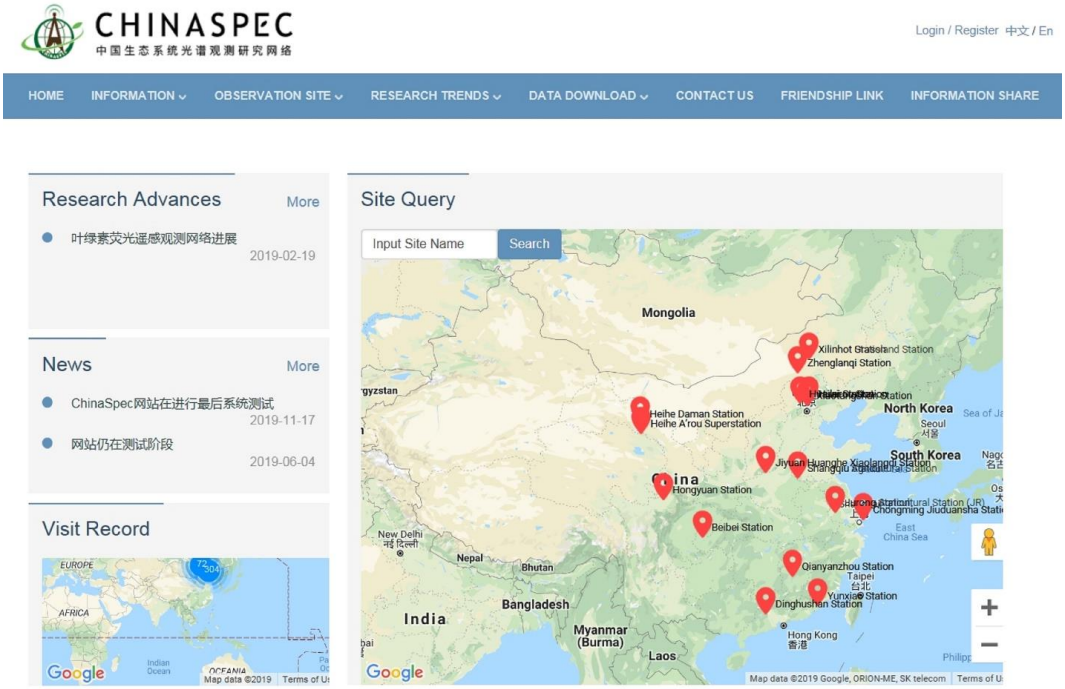

Figure 4. Website of ChinaSpec (http://chinaspec.nju.edu.cn). Introduction, data sharing and other information are provided through this website.

The data usage polices for ChinaSpec is similar to that for FLUXNET dataset (especially the FLUXNET2015 Dataset). The use of spectral data in ChinaSpec will follow “the fair use policy” (https://fluxnet.fluxdata.org/). In other words, the ChinaSpec datasets are open and freely available for scientific and educational purposes by any registered user after acceptance of a proposal submitted to the steering committee. That is, data users submit a proposal on the intended use of the data before they download the data; this intended-use statement will be emailed to the data producer(s) of the sites. This policy means that “(1) data producers are informed of who uses the data and for what purpose and (2) that proper acknowledgment and citations are given to all data used in a peer reviewed publication, via the following protocols: providing a co-authorship to the site PIs or at least a citation of a publication for each site”. It is requested that every publication specifies each site used with the data-years used and brief acknowledgment for funding (if provided by the PI) in the text. We recommended the users to contact the site PIs before publishing to avoid potential misuse or misinterpretation of the data.

In particular, if a work is based on the SIF data from only a few sites, it is strongly recommended to contact the site PI about co-authorship or proper acknowledgment for their contribution.

The distribution of the data for each site will be shared after the first publication or 2-3 years later after data collections. At this stage, the dataset consists of metadata of each site, vegetation indices (e.g., NDVI, EVI, and PRI depending on sites), retrieved far-red SIF (760 nm) with two methods (3FLD and SFM) after data quality control. The temporal scale of the dataset is half hourly, which is processed from high frequency raw data (~1 minute for spectral data). Error/uncertainty estimations on retrieved SIF will be also included in the dataset in the future. Since the year of 2019, we have distributed the spectral dataset including reflectance and SIF for 1-2 years from 6 sites. The rest of the spectral dataset will be regularly updated with data from new site years.

4 The usefulness of networking SIF observations

Field spectral and SIF measurements collected in ChinaSpec are not only essential for the integration of optical remote sensing and EC flux data across space and time, but also for investigating the dynamics of canopy SIF and its link to GPP across multiple spatial and temporal scales. These continuous ground-based measurements of SIF will also benefit validation of fluorescence models and satellite SIF retrievals.

4.1 Characteristics of canopy SIF and its link to GPP across multiple ecosystems

There are growing interests on how SIF changes with radiations and GPP across different ecosystems. Among the sixteen sites in the ChinaSpec network, eight sites were selected as an example to investigate the relationships of SIF with photosynthetically active radiation (PAR) and GPP at diurnal scale (Figure 5). SIF generally varied with both PAR and GPP across these sites at diurnal scale, which indicates that SIF and GPP were both driven by PAR under the clear sky conditions. For the broadleaf forest, SIF mostly varied with GPP though SIF and GPP obviously decreased in the afternoon even PAR level was higher than that in the morning. At seasonal scale, the results from four sites also show that the seasonal dynamics of SIF and GPP were generally consistent during the growing season, while NDVI was generally stable (Fig. S1 in Appendix). In particular, SIF captured the increase of GPP at the start of the growing season (DM) and decreased at the end of the growing season (SQ), when PAR remained at a high level. On the other hand, NDVI increased with GPP and SIF at the beginning of the growing season, but maintained high values after SIF and GPP decreased after day 240. It then started to decline until SIF and GPP approached zero, possibly contributing to the fact that plant LAI remained stable until the very end of the growing season. These results demonstrate the potential of continuous SIF measurements for understanding diurnal and seasonal canopy SIF variations across different vegetation types, and also highlight the importance of networking on SIF measurements.

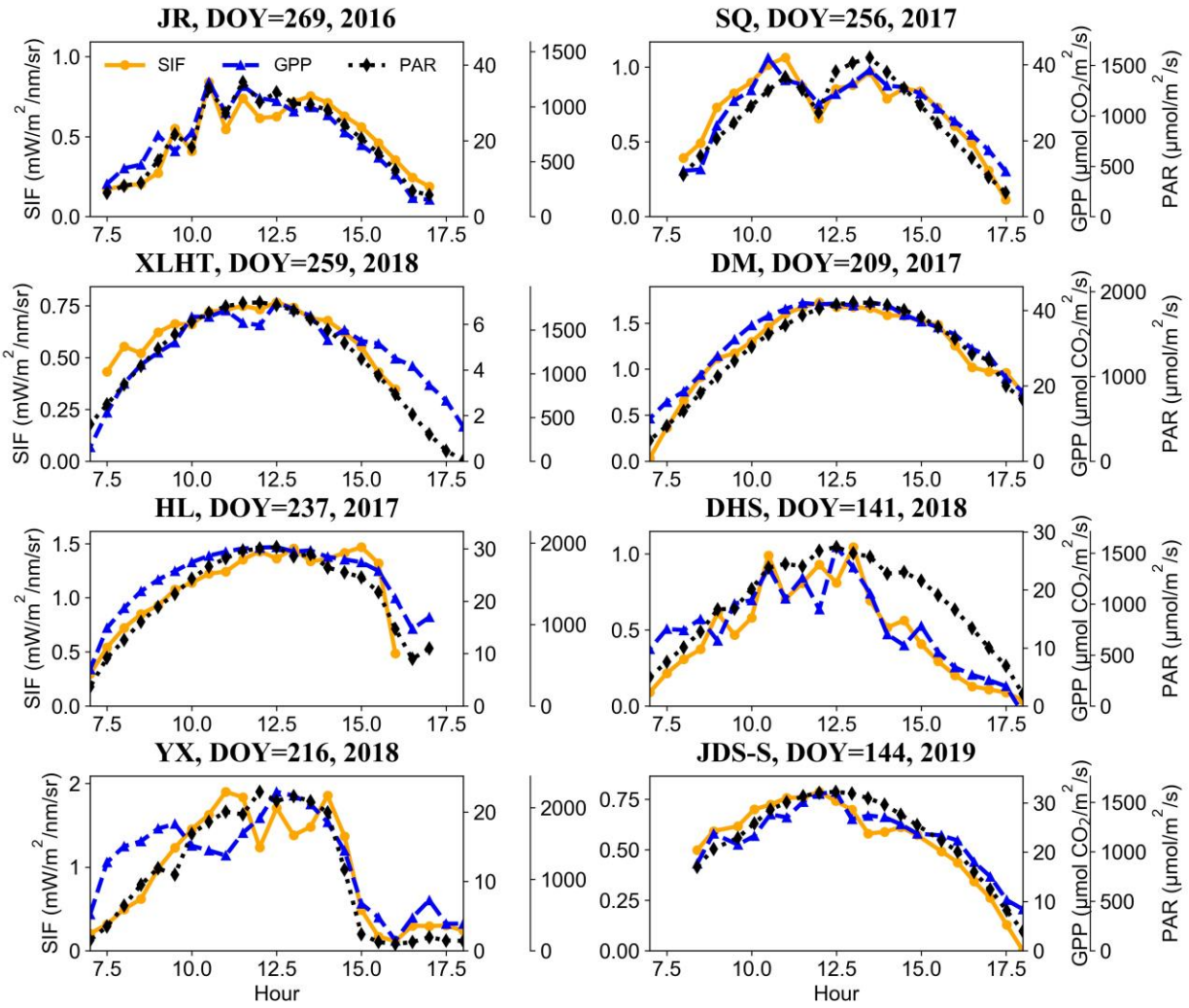

Figure 5. Diurnal variations of SIF, PAR, NDVI and GPP in a clear-sky day at eight SIF sites in ChinaSpec. For each site, we chose one clear-sky day for illustration. Site names are identified in Table 1.

Different relationships between SIF and GPP have been reported in different ecosystems at the seasonal scale (e.g., Yang et al., 2015; Damm et al., 2015; Wieneke et al., 2018; Yang et al., 2018a; Nichol et al., 2019; Li et al., 2020). At the diurnal scale, however, it is not clear how this relationship varies across different vegetation types. With the observations from ChinaSpec, we further analyzed the relationship between SIF and GPP at diurnal scale across different vegetation types. Figure 6 shows that there are also significant diverse slopes of relationships between SIF and GPP but comparable relationships between SIF and PAR at diurnal scale across different vegetation types. The inconsistent relationships between SIF and GPP across different ecosystems may be attributed to different canopy structures. The regression slopes of SIF with PAR from different sites have less variations. Additionally, SIF is also affected by escaping probability due to multiple scattering in far-red region. This indicates the necessity to expand SIF observations covering a variety of ecosystems to investigate and improve the ability of SIF for monitoring photosynthesis. With the growing SIF observations in ChinaSpec over multiple ecosystems, further synthesis work could be done for better understanding the link between SIF

and GPP at different temporal and spatial scales by combining with satellite and drone-based SIF measurements.

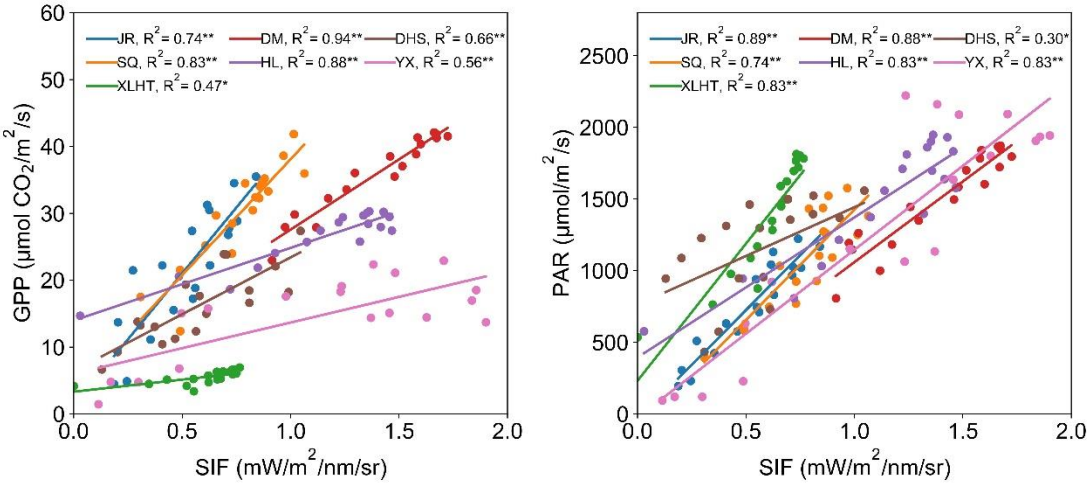

Figure 6. Diurnal relationship between SIF and GPP across multiple sites from one-day measurements under clear-sky conditions. Site names are defined in Table 1.

4.2 Validation of fluorescence models with ground-based SIF observations

Development and validation of fluorescence models are reliant on observational data. Here we refer to examples of the utility of ChinaSpec data for validating these models. During recent years, several fluorescence models have been developed for the purpose of canopy radiative transfer of SIF. A widely-used model is the Soil-Canopy Observation Photosynthesis and Energy fluxes (SCOPE), which is typically used to simulate SIF at the site level (Van der Tol et al., 2009). To conduct global SIF simulations, several terrestrial biosphere models have been also coupled with fluorescence model (e.g., Lee et al., 2015; Qiu et al., 2019). For example, an efficient scheme accounting for the canopy scattering of SIF has been developed and implemented into the Boreal Ecosystem Productivity Simulator (BEPS-SIF) (Qiu et al., 2019).

We use continuous ground-based SIF observations from three sites (JR-rice, SQ-maize and XLHT-grassland) in ChinaSpec to compare with SIF simulations by SCOPE and BEPS-SIF model (See details in the Appendix A for model setup). Figure 7 shows the scatter plots between observed SIF and simulated SIF from SCOPE and BEPS-SIF at both hourly and daily scales for one year's data. For all the three sites, SIF simulations from two models are significantly correlated with ground-based observations, though the relationship between BEPS-SIF simulation and observation is slightly scattered. This result demonstrates that these two models are effective in simulating SIF for different vegetation types at both hourly and daily scales. The equally good performance of BEPS-SIF with SCOPE also illustrates its effectiveness for regional and global SIF simulations. This comparison between observations and simulations demonstrates the potential of continuous ground-based SIF observations to validate fluorescence models at multiple temporal scales.

Ground-based SIF measurements could also feature in the development of new model components. For example, SIF measurements at a subalpine forest in Colorado are used to account for sustained NPQ in the SIF model, which largely improves the seasonal variations of

SIF simulations for evergreen conifer forest (Raczka et al., 2018). With more data available in ChinaSpec, the synergy of ground-based SIF data and fluorescence models will help to improve mechanistic understanding of photosynthetic activity and SIF at different temporal scales (i.e, diurnal to seasonal), which is important for constraining large-scale simulations of terrestrial carbon cycles from satellite SIF data.

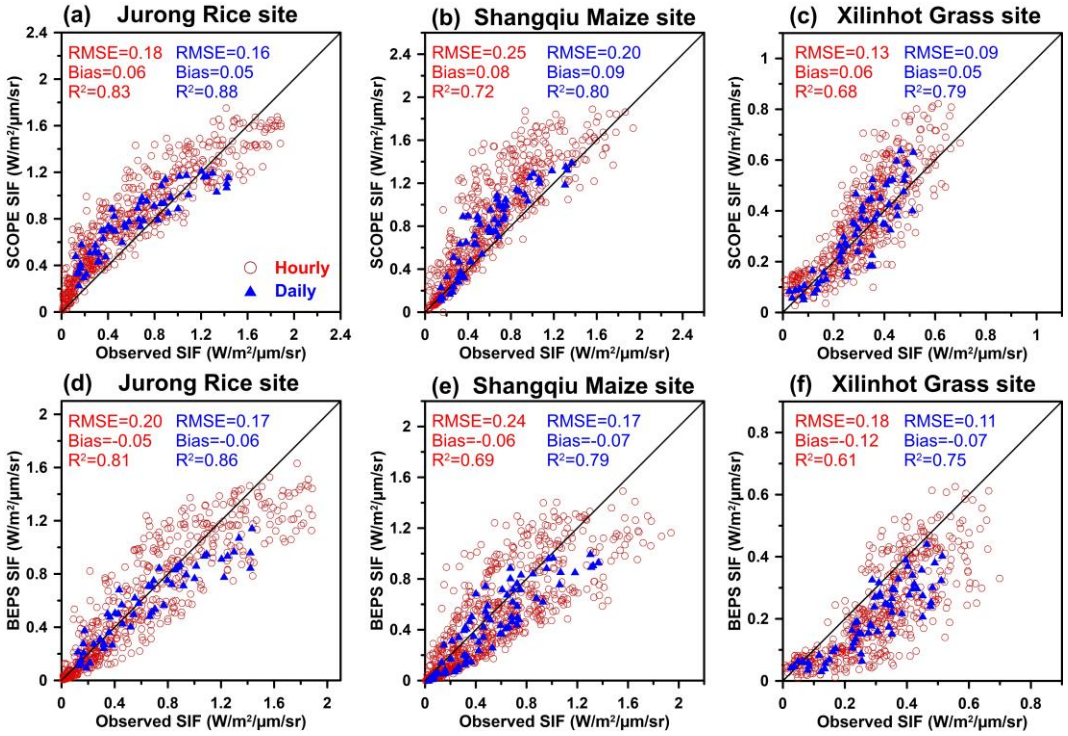

Figure 7. Validation of the fluorescence models using ground-based SIF measurements for (a-c) SCOPE model and (d-f) BEPS-SIF model. Site names are identified in Table 1.

4.3 Validation of satellite SIF observations at the site scale

Validation against ground-based SIF observations is necessary for satellite SIF products. Continuous ground-based SIF measurements in ChinaSpec over multiple vegetation types provide opportunities for direct comparison and evaluation of satellite products. In particular, the fine spatial resolution of OCO-2 and TROPOMI SIF have facilitated the comparison with ground-based measurements, though it is still challenging due to spatial mismatch. Here, five relatively homogeneous sites in ChinaSpec, including four croplands (JR, HL, DM, and SQ) and one grassland (XLHT), are chosen to compare with SIF retrievals from TROPOMI and OCO-2. They have overlap with the swath from both OCO-2 and TROPOMI. Land cover around each site is shown in Figure 8, which also shows the available observations from OCO-2 from 2014 to 2018. To compare with ground-based observations, both TROPOMI and OCO-2 SIF observations were averaged from all available data within a 50 km-buffer around each site (red circle in Figure 8).

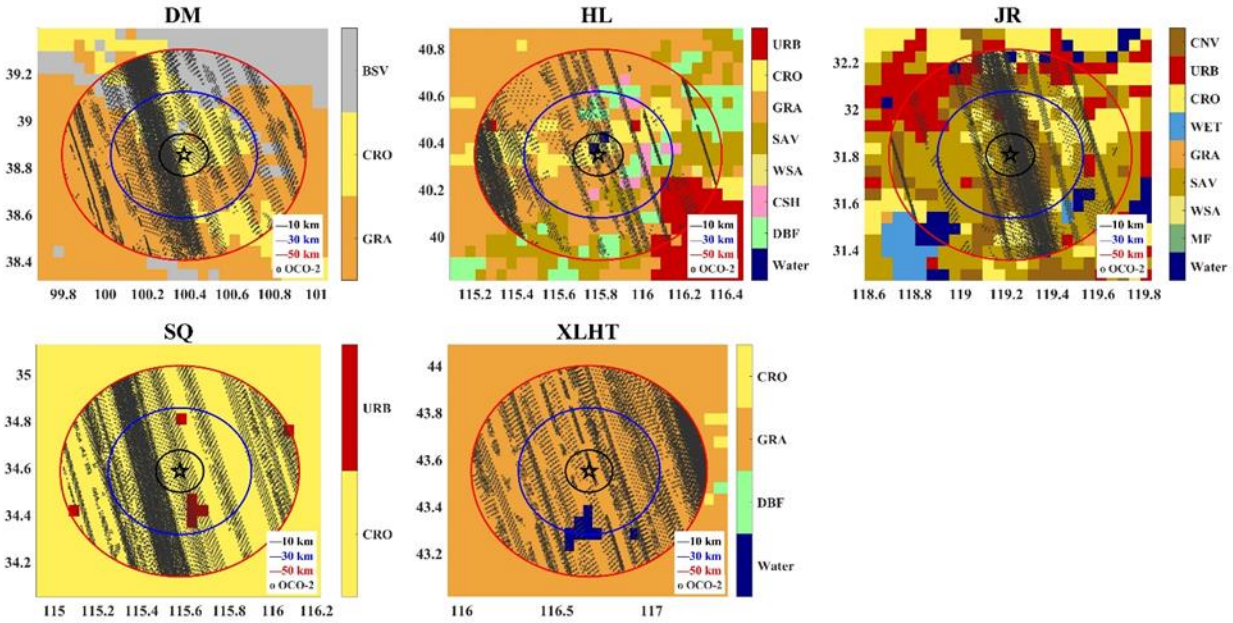

Figure 8. Surrounding land cover and available OCO-2 observations with buffers of 10 km, 30 km and 50 km radius at five SIF sites (DM, HL, JR, SQ and XLHT). The base map is land cover type from MODIS Land Cover product (MCD12C1 v6). Black dots are OCO-2 overpasses at each site from 2014 to 2018.

Figure 9 displays seasonal variations of SIF retrievals from ground-based observations and two satellite products. Note that ground-based SIF values of each day are averaged at the overpass local time of ~1:30 pm of OCO-2 and TROPOMI. As for OCO-2 SIF with a coarse temporal resolution (16 days), multi-year (2014-2018) mean data are used as the climatic mean SIF. Overall, both OCO-2 and TROPOMI SIF show seasonal consistency with ground-based SIF measurements, capturing the timing and amplitude of seasonal features over a variety of vegetation types. This is further confirmed by the correlation between TROPOMI and ground-based SIF (Figure 9). Significant relationships ($p<0.001$) were observed for all sites except for HL during the growing season of wheat. The correlation (R^2) varied across different sites, ranging from the minimal of 0.34 at XLHT to the maximal of 0.75 at JR. Considering that there are still mismatch of the footprint between satellite and ground-based measurements; such direct comparison demonstrates the potential of ground-based SIF measurements in ChinaSpec for validation of satellite SIF data.

However, this rough and direct comparison also exemplifies the challenges for the validation of different satellite SIF observations with ground-based SIF measurements. Lesser agreement (i.e., HL and XLHT) might be due to the mismatch of footprints between satellite SIF and ground-based measurements of SIF. It is important to filter out uniform vegetation, even for mostly homogeneous areas. It would also be worthwhile to explore the synergy of UAV-based and ground-based SIF systems to validate/evaluate satellite data across sensors over multiple sites in the network. The advances in UAV-based SIF systems (MacArthur et al., 2014; Bendig, et al., 2018) offer unique opportunities for upscaling ground-based SIF measurements to satellite level observations.

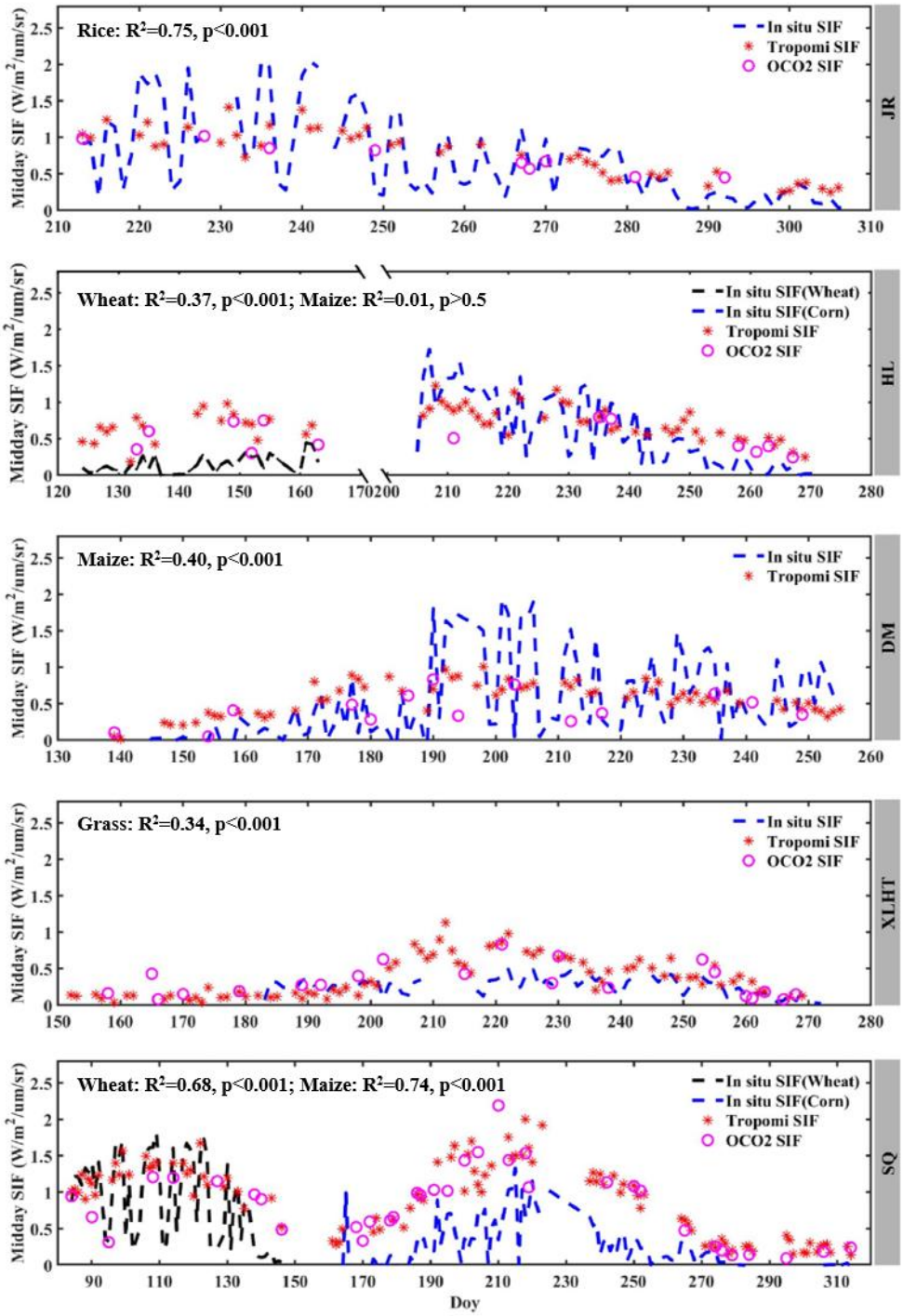

503

504 **Figure 9.** Comparison of seasonal variations of ground-based and satellite (TROPOMI and
505 OCO-2) SIF observations at five SIF sites. The correlation coefficient (R^2) in each subplot is
506 between TROMPO and ground-based SIF measurements. Site names are identified in Table 1.

507

5 Outlook and challenges

The dataset shared by ChinaSpec network will promote the developments of the methods and data quality of spectral measurements in China, and enable a new perspective of integrating spectral and EC measurements with the aim to increase the quality of the research and the collaboration on ecology and optical remote sensing communities. During the development of ChinaSpec network, we have also encountered a number of opportunities and challenges for integrating EC flux and remote sensing data.

5.1 Implications for linking SIF with EC flux measurements

Understanding the spatiotemporal dynamics of the carbon cycle and its response to climate change is still one of the great challenges. EC flux networks have played a unique and valuable role in quantifying ecosystem carbon exchange at landscape scale. Satellite remote sensing data has been widely used to scale EC flux data in space and time. In particular, the recent breakthrough in remote sensing of SIF has stimulated the research in monitoring terrestrial photosynthesis at large scale. However, a direct comparison is difficult between remotely sensed and ground measurements due to the differences in sampling scales in space and time. An opportunity to investigate the ability of SIF to monitor biosphere-atmosphere carbon exchange with synthetic spectra and carbon flux observations under all weather conditions benefits from the development of high-resolution spectroscopy technique (Porcar-Castell et al., 2015). In this context, ground-based spectral and SIF measurements have comparable temporal and spatial sampling scale to that of EC flux measurements, which could facility the integration of remote sensing and ground-measured fluxes. Overall, ground-based SIF measurements are essential for upscaling remote sensing and flux data across space and time. The ChinaSpec network is established with this goal in China and is also aligned with the long-term plan for Chinese terrestrial ecosystem science (Yu et al., 2010). The development of the ChinaSpec network within the framework in ChinaFLUX network (Yu et al., 2006; Yu et al., 2010) will help bridge the integration of EC flux measurements and remote sensing.

A primary ChinaSpec goal is to improve the understanding of links between SIF and photosynthesis or GPP across different vegetation types and scales. Understanding the linkage of SIF-GPP is fundamental to monitoring global photosynthesis from satellite SIF data. Over the last decade, most efforts to investigate the relationship between SIF and GPP derive from the satellite SIF data (e.g., Guanter et al., 2014; Sun et al., 2018). Ground-based SIF measurements have also recently emerged as a useful tool to study the temporal and spatial variability of SIF and its link to GPP at the site scale (e.g., Yang et al., 2015; Damm et al., 2015; Nichol et al., 2019; Li et al., 2020). However, such analyses mostly focus on single site in different ecosystems. Strong linkages between SIF and GPP have been found, but the form of the relationships varies (non-linear or linear) depending on vegetation types and spatio-temporal scales (Mohammed et al., 2019). Furthermore, it is still unclear whether SIF is more related to GPP or APAR for different plant functional types or species (e.g., Yang et al., 2018b; Magney et al., 2019). Thus, establishing a network of ground-based SIF observation systems is important to fully characterize the relationship between SIF and GPP by obtaining synchronous SIF continuous observations and CO_2 flux measurements across different terrestrial ecosystems and to understand photosynthetic activities of terrestrial ecosystems. A synergy of SIF and EC flux measurements in a network such as ChinaSpec could benefit the analysis of SIF and flux data for a cross−site syntheses because relative standardized instrumentations and field-setups (see

552 section 2.1 and 2.2) are employed in ChinaSpec. As shown in Figure 6, a cross-site synthesis
553 sheds light on the controls of SIF- GPP linkages at diurnal scale in different vegetation types.
554 With ongoing continuation of SIF observations from different sites in ChinaSpec, it is possible to
555 study not only the short-term (diurnal and seasonal) but also inter-annual variability of SIF and
556 its linkage to GPP. Furthermore, long term ground-based SIF measurements have the potential to
557 be used to investigate the diurnal and seasonal changes in GPP across different biomes, canopy
558 structures and environmental conditions, which is not available for the current satellite due to the
559 discrete temporal samplings and instrumental difference among different satellites.

560 Long-term and continuous SIF measurements in ChinaSpec could also benefit the utility
561 of ground-based measurements to upscale to regional scales. Although satellite SIF has shown to
562 be a good proxy for GPP, the existence of scale mismatch between satellite SIF and flux tower
563 GPP hinders the full use of SIF to constrain GPP at the global scale. Meanwhile, we are working
564 with the SIF communities in Europe and USA, and will link ChinaSpec to other global SIF
565 networks. Similar to the global network of FLUXNET, this SIF network has the potential to
566 become an important ecological research tool for large-scale photosynthesis monitoring,
567 especially when made concurrently with EC flux observations. More importantly, the temporal
568 match between ground-based SIF measurements and flux data benefits the modeling and
569 validation of the linkages derived from the satellite data, which could improve the upscaling of
570 flux measurements from the footprint to the large scales. By integrating SIF and EC
571 measurements over space and time, we could also assess ecosystem function to a number of
572 biophysical forcings such as temperature, water, light and phenology. Overall, these high
573 frequency ground-based SIF and reflectance can complement the long-tern EC carbon and water
574 flux measurements, and help to bridge ground-based observation and satellite SIF products for
575 carbon flux prediction over a variety of ecosystems.

576 In addition, the regional network of ChinaSpec could also contribute to the calibration
577 and validation of satellite SIF products, and help to resolve issues that derive estimates of large-
578 scale GPP directly from satellite data. Currently, there are a number of spaceborne sensors with
579 high-spectral resolution which enable the global retrievals of SIF at regional and global scales,
580 including GOSAT, GOME-2, OCO-2, and TROPOMI (Frankenberg et al., 2011; Joiner et al.,
581 2013; Köhler et al., 2018; Sun et al., 2018). Airborne high resolution imaging sensors are also
582 available for retrievals of SIF at landscape scale (e.g., HyPlant and CFIS) (Rascher et al., 2015;
583 Frankenberg et al., 2018). Therefore, it is urgent to develop ground-based measurements of SIF
584 in parallel to validate the accuracy of SIF retrievals from satellite or airborne platforms. Most
585 current satellite SIF is measured at a certain time of a day (e.g., GOME-2 local overpass time is
586 around 9:30 a.m.). Therefore, the validation of satellite-based SIF can provide robust information
587 on regional to global-scale plant photosynthetic function and provide important information for
588 ecosystem photosynthesis monitoring from satellite remote sensing. Concurrently, comparisons
589 with ground-based SIF also play an important role in the calibration of SIF models (e.g.,
590 SCOPE). In addition, the information of red SIF retrieval has been investigated from ground-
591 based SIF measurement but is not available for most current satellite SIF observations. Since red
592 SIF contains more information of the photosystem II, the knowledge obtained from ground-
593 based measurements will help the use of red SIF from satellite mission (e.g., FLEX) to achieve a
594 combination of red SIF and far red SIF, which is important to understanding the mechanisms of
595 SIF emission by vegetation.

5.2 Standardization of instrumentation and data process

The main challenge to the establishment of an optical measurement network, as in any other network, is the standardization and comparability of measurements across sites. The standardization is especially important and challenging for the ground-based SIF measurements across different vegetation types since optical measurements are more complicated. One of the lessons from the development of ChinaSpec is that standardization is the first priority for a successful network of SIF measurements. Lack of standardization of optical sensors and sampling methods will make it difficult to directly compare measurements across sites (Porcar-Castell et al., 2015; Gamon, 2010).

Continuous automatic canopy SIF observation in the field is not as straightforward as are EC flux measurements. Our ability to conduct continuous SIF observations is due to the development of stable sensors and systems with high spectral resolution and SNR to measure high-frequency spectral signals (e.g., Aasen et al., 2019; Parazoo et al., 2019). During the last decade, a number of SIF instruments have been developed for ground-based measurements. However, the standardization of SIF observations systems is still in its early stage compared to EC flux instruments. In the ChinaSpec network, we propose the use of the relatively uniform instrumentations (at least the same sensor) to produce comparable spectral data. Though different SIF systems are used at different sites, the custom designed spectrometers, light path and spectrum sampling methods are very similar for ground-based continuous spectral measurements in ChinaSpec (see Section 2.1). The advantage of these spectrometers is the thermal stabilization of the detector, and with high SNR (~1000:1). This reduces the uncertainties in making cross−site comparisons. However, there are still discrepancies in the spectral range and resolution among the SIF systems at different sites. In the future, we suggest a more standardized systems with a spectral range of 650-800 nm to be used to improve data quality, and benefit the comparison of SIF data across sites. Furthermore, we suggest a complementary VNIR spectrometer (~400-1000 nm) in these systems to collect broadband reflectance for deriving VIs. It is also useful to have complementary biophysical measurements (leaf chlorophyll, LAI, etc.).

Field setups and protocols are also critical for ground-based optical measurements, especially for hyperspectral measurements needed to retrieval SIF. Due to the very dynamic nature of SIF, it needs particular and careful consideration in the measurement setups and protocols. Much progress has been made in applying SIF systems for SIF observations at flux sites over the past decade (e.g., Cogliati et al., 2015; Yang et al., 2015; Grossmann et al., 2018; Aasen et al., 2019). Retrieving SIF at the canopy level in the field requires synchronously measured incoming and outgoing solar irradiance. In general, incoming solar and outgoing canopy radiation should be acquired as simultaneously as possible using the same sensor to avoid spectral shifting from two sensors. Several instrument configurations can be applied to ground-based SIF measurements to collect incoming and outgoing solar radiation: hemispherical-conical and bi-hemispherical configurations (e.g., Porcar-Castell et al., 2015; Yang et al., 2015; Gu et al., 2019). At the current stage of ChinaSpec, we utilized the hemispherical-conical configurations with a nadir view at a single fixed point for continuous measurements at all the sites. We suggest in ChinaSpec that solar irradiance measurements use a cosine diffuser for continuous observations. For canopy radiance, a conical foreoptic (bare fiber) is used to measure upwelling radiance from canopy which is installed at nadir. The SIF systems are generally installed on the flux towers or close to the towers to maximize the synergy of SIF and EC flux measurements. The heights above the canopies are dependent on the vegetation structure and tower

infrastructures at each site. An appropriate height that instruments are installed is suggested to represent the footprint of EC flux measurements. Overall, we propose consistent measurement setups and protocols at this stage in ChinaSpec, which could help avoid any possible uncertainties due to instrumentation and setups. However, an in-depth discussion on the proper protocol of SIF measurement is still needed since the science of SIF observation is still under development.

The last important aspect in a network is the standardization of data post-process and SIF retrieval. Reliable retrievals of SIF need careful quality checks of the spectral data before analysis. This is particular important for the automated field SIF systems measurements under diverse environmental conditions. Though data collection and storage are conducted in different ways in ChinaSpec, the spectral information, including raw DN, IT and DC, are all recorded for post-processing. The same data processing and analysis techniques are also needed to better standardize the SIF measurements across sites. At the current stage of ChinaSpec, we adopt the data post-process chain introduced by Cogliati et al. (2015). As mentioned in Section 2.3, the raw data should be corrected (dark current), calibrated (radiometric and wavelength calibration) and non-linearity corrected, as well as data quality check following a standard procedure for reflectance calculation and SIF retrievals (Cogliati et al., 2015). This is necessary for processing such large amounts of spectra from unattended automated systems to exclude low-quality data due to illumination changes (cloud overpass), high solar zenith angle, and instrument saturation. As for the methods of SIF retrieval, we propose the use of SFM as the main retrieval algorithms with 3FLD as a backup in the current stage of ChinaSpec. The SFM approach is one of the most reliable SIF retrieval algorithms for ground-based SIF measurements (Cendrero-Mateo et al., 2019). Thus, we suggest that the output data for sharing at least consists of solar and canopy radiation, PAR, reflectance and SIF retrievals using 3FLD or SFM in ChinaSpec. Ancillary metadata are also necessary to describe the information on the site, observation system and data structure, etc. Since SIF retrievals are also influenced by atmospheric conditions, information on diffuse/total radiation, air temperature and pressure could be helpful for atmospheric correction. Overall, it is important to conduct quality checks and provide quality flags in the metadata for a better interpretation of SIF measurements across sites.

5.3 Ongoing challenges and future prospects

Though substantial progress has been made on networking the ground-based continuous SIF observations, we have identified several challenges and opportunities during the development of ChinaSpec. These includes standardization of measurement protocols and data processing, footprint-representativeness of measurements, integration with EC flux measurements, and connections with other regional network. This standardization will further advance our understanding of SIF signal and its link to photosynthesis by addressing these issues in the near future.

5.3.1 Issues in measurements protocols at EC sites

During the last decade, significant progress has been made for the development of instrumentation and protocols in SIF measurements. However, the SIF community still lacks a consensus on the standardization of SIF measurement protocols. Though we suggest the use of more consistent instruments and field setups in ChinaSpec, independent PIs may still adopt different solutions for SIF measurements without following a set of general guidelines. There are still some open questions that link to standardization of SIF instrumentation and protocols. The

discussion in Sections 5.2 are considered as a starting point, but more research is needed in this direction. We identified several areas that still need further work.

Of particular concern is the radiometric and spectral calibration of SIF systems. This is a new challenge to calibrating the automated SIF sensors on a continuous basis at the flux sites. Since SIF retrievals need measurements of absolute solar irradiance and vegetation radiance, the absolute radiometric calibration becomes especially critical to derive reliable and reproducible SIF retrievals. Due to its continuous measurements over months to years, a regular onsite calibration is definitely needed for the sensors to avoid drift over time. We find that some of the SIF instruments were rarely calibrated over a year even though we suggest an onsite calibration at approximately every 3 months. In addition, wavelength calibration of spectrometers are also important to ensure that SIF retrievals are using the correct wavelength regions. Spectrometers are initially calibrated by the manufacture and should be periodically recalibrated to correct bias from true variations by sending them back to the suppliers. We suggest that the QEPro used in the SIF instruments are recalibrated after one year of purchase by the manufacture. This regular recalibration was rarely done in ChinaSpec. Thus, the stability of such sensors over time in the field needs further investigation. We recommend routinely both spectral and radiometric calibration of the instruments at least once per year at the beginning of the growing season. Overall, any failure of regular radiometric and spectral calibration of these SIF systems may result in non-reproducible and non-comparable data which is of limited scientific value. Apparently, there is an urgent need for more close collaboration between SIF scientists and industry to foster the technological improvements. Such collaborations could help develop more reliable and standardized SIF instruments.

There is also a need to develop more stable SIF retrieval methods and data quality control standards. The retrieval methods used in ChinaSpec, SFM and 3FLD, are based on the FLD principle using O_2 A and O_2 B absorption features which are easily affected by atmospheric scattering, surface pressure and temperature conditions. The atmospheric effects between the SIF sensors and the observed canopy needs more attention. A few studies have suggested the necessary of atmospheric correction on SIF retrievals even though there are only a few meters between canopy and sensor (Sabater et al., 2018; Aasen et al. 2019). Considering that some SIF systems are mounted on flux towers at greater than 10 m above the canopy, we recommend the use of an atmospheric correction routine before SIF retrievals (Liu et al., 2019). Otherwise, a SIF retrieval algorithm based on Fraunhofer line such as singular vector decomposition (SVD) could be used to provide tolerance for atmospheric scattering effects. At the present, however, we still do not have a guaranteed method for SIF retrievals which can be used for all sky conditions. In addition, the retrieval of red SIF (F_{687}) at the O_2 B band is more challenging, and a systematic assessment of the current SIF method in the near future is needed to ensure a stable approach for red SIF. Clearly, there is still much work needed on SIF retrievals and data quality control on the ground-based SIF measurements for future research.

5.3.2 Footprint match of SIF and EC fluxes

Another challenge for the synergy of SIF and EC flux measurements research involve effectively integrating SIF and EC flux measurements. There is still debate on how to deal with the effect of SIF vs. flux footprint mismatch from a point of view of ground-based measurements. The current continuous SIF measurements can temporally match well with EC flux data. However, the issue of footprint mismatch is critical between SIF and EC flux measurements. It is well known that the EC flux footprints vary with wind direction, atmospheric

stability, measurement height and canopy structure. On the contrary, the SIF systems are usually deployed in a fixed direction (a bare fiber with nadir) on top of a flux tower, which generally have a footprint of a few to a tenth of a meter squared. This will obviously result in footprint mismatch with flux observations, and miss the peak contribution area of the flux. In sites with homogenous canopy (e.g., crop, grassland), the spatial representativeness of SIF data may not be a critical issue. In places with heterogeneous vegetation like savanna, however, characterization of the footprint match could be critical for the joint use of SIF and flux data.

This footprint mismatch between optical and flux observations clearly points out the need for better SIF observations or post-processing to create representative SIF signal of flux footprints. The influence view-geometry and canopy structure are also needed to account for the interpretation of SIF, especially at diurnal scale. This is due to the distribution of light throughout the canopy (i.e., the classic surface BRDF problem). A few studies have reported the strong angular dependence of SIF emissions on sun-canopy geometry and canopy structure from ground-based measurements (Pinto et al., 2017; Zhang et al., 2020). Thus, we find that new tools/protocols are needed to address these issues. One option is the use of a multiangular SIF system, which can collect spectral measurements over a circular area surrounding the flux tower. For example, Zhang et al. (2020) recently presented an automated multi-angle SIF system (Multi-Fluo) capable of measuring the angular dependencies in measurements of top-of-canopy SIF in crops. The Multi-Fluo system also uses QEPro (FWHM of ~0.3 nm, Ocean Optics, Dunedin, FL, USA) to automatically acquire spectra with different viewing angles of the canopy that cover different areas around a flux tower. Some correction of the directional SIF signal could be done to derive total canopy SIF emission by combining canopy reflectance data (Yang and van der Tol, 2018; Liu et al., 2019; Zeng et al., 2019; Zhang et al., 2019).

The other option is to use the bi-hemispherical measurements with a cosine corrector with FOV of 180° (Zhang et al., 2019; Gu et al., 2019). The bi-hemispherical configurations could enlarge the field of view to represent the average condition of the canopy and also reduce the signal from non-vegetation factors. These systems could measure a large area around the flux towers, which make them a valuable solution to address footprint variability. In the future, we recommend conical measurement of radiance for homogeneous canopy (e.g., crop and grassland), and hemispherical measurement for heterogeneous canopy (e.g., forest, savanna) (Balzarolo et al., 2011; Porcar-Castell et al., 2015; Gu et al., 2019). In addition, cost-affordable UAV-based SIF instruments (e.g., Piccolo, MacArthur et al., 2014) are also unique systems available to quantify the footprint variability, since they have more flexibility and capacity to measure the same canopy from different heights. This will be especially valuable in investigating the different sources of error to upscale from ground-based SIF measurements to satellite pixel level. However, further considerable work is still needed on this subject and our understanding of how to address this scale issue at the flux sites requires more attention.

5.3.3 Towards a global SIF network

Through the integration of ground-based SIF and EC observations in a network, we are able to deepen our understanding of the controlling mechanisms of the biosphere-atmosphere carbon exchange. In the next few years, we anticipate a continuing expansion of ChinaSpec to more vegetation types/sites. Two more sites, Naqu site in Tibet (31.64N, 92.01E) and Shihezi in Xinjiang (44.91 N, 86.16 E), are starting the SIF measurements in 2020. In particular, the Naqu site is located in Northern Tibetan Plateau and with an altitude of 4,600 m and a vegetation of typical alpine meadow dominated by *Kobresia pygmaea* (*K. pygmaea*) (Zhu et al., 2020). These

sites make ChinaSpec very unique in SIF measurements in the highest landscape. Some future projects have already been discussed for deploying automatic SIF systems over more forest, wetland and alpine meadow sites in ChinaFlux. As the network is growing with more sites in ChinaSpec and other regional network (Yang et al., 2018a; Aasen et al. 2019; Parazoo et al., 2019), we could expect a global ground-based SIF network similar to the global network of FLUXNET in the near future. Yet, there is still tremendous work needed to accomplish this coordinated goal. The effort could benefit from communication and collaboration between the SIF community and EC flux scientists. A relevant platform for communication among different communities would help to promote the development of such a global SIF network. Apparently, SIF observations alone cannot fully show the advantage of SIF for photosynthesis and carbon cycle research (Gu et al., 2019). Concurrent SIF and EC measurements could resolve some challenges in global photosynthesis estimation. However, much effort is still needed to establish a global standard for measurement protocols and data processing. Further work should investigate how different approaches in different regional networks can be consolidated/synthesized in a meaningful way to gain the full SIF picture. It can be foreseen that a regional/global joint long-term measurements of SIF and EC flux are very useful for improving our understanding of biosphere-atmosphere interactions. Collaboration from data scientists is also needed for studies that can fully utilize the rich information contained in the large amount of ground-based SIF data that is and will be available.

6 Summary

An automatic spectral observation system has been used to continuously measure ground-based canopy reflectance, especially SIF, which is an efficient approaches for monitoring the carbon budget of terrestrial ecosystems. The network of ChinaSpec was established to conduct ground-based SIF measurements using automated instruments across various vegetation types in China. The network currently consists of 16 sites including six cropland sites, four grassland sites, four forest sites and two wetland sites. Here, we specifically describe the details of instrument configurations, data collection and processing procedures, data sharing and utilization protocols. Based on data acquired from sites in last two years, we show examples how the SIF observations can be used to track vegetation photosynthesis from diurnal to seasonal scale, to validate the fluorescence models and satellite SIF products (e.g., from OCO-2 and TROPOMI). ChinaSpec is dedicated to facilitate integration of spectral and flux measurements for better monitoring and prediction of carbon exchange between the atmosphere and biosphere, and benefits both remote sensing and ecology research communities. Still, there are many challenges in expanding the network and in reaching a standard protocol from data acquisition, processing to utilization. This necessarily requires broader collaborations from interested researchers or groups to advance this research area.

Acknowledgments

This research was supported by the National Key R&D Program of China (2019YFA0606601, 2017YFC0503800), and the General Program of Natural Science Foundation of China (41671421). We would thank Dr. Zhongyang Li, Dr. Hezhou Wang and other researchers from National Agro-Ecological Observation and Research Station of Shangqiu, Henan, China for the field measurements. These students involved in the data collection were also acknowledged. We would also like to thank Prof. Mark Nearing at University of Arizona for the English correction. We would also like to acknowledge the NASA Earth Science Data Systems program for the MODIS (https://e4ftl01.cr.usgs.gov/MOTA/MCD12C1.006/) and OCO-2 products (ftp://fluo.gps.caltech.edu/data/OCO2/sif_lite_B8100/). The TROPOMI SIF data providers, Prof. Philipp Koehler and Prof. Christian Frankenberg, were also acknowledged (ftp://fluo.gps.caltech.edu/data/tropomi/ungridded/SIF740nm/). We also greatly appreciate the ChinaFLUX for providing EC flux data (http://www.cnern.org.cn/data/meta?id=141840).

Appendix A. Information on the model setups.

SCOPE is a vertical (1-D) integrated radiative transfer and energy balance model and has been widely used for simulating both photosynthesis and chlorophyll fluorescence processes. In this model, the canopy is divided into many elementary layers and the leaf angle is treated as 36 leaf azimuth classes and 13 discrete leaf zenith inclinations. SCOPE can simulate the fluorescence emitted from all the leaves and canopy-leaving fluorescence by considering the re-absorption and scattering processes within the canopy. The latest version of SCOPE (v1.73) is used for the simulation of SIF observed at the top of the canopy. The meteorology forcing data for SCOPE simulations include incoming shortwave and longwave radiation, air temperature, surface atmosphere pressure, atmospheric vapor pressure, and wind speed.

The BEPS model is an enzyme kinetic two-leaf model, which has been used to simulate water and carbon fluxes for different vegetation types at both site and global levels. An efficient scheme to account for the canopy scattering in a SIF model has been developed and this mechanistic representation of SIF is coupled to the BEPS model. The BEPS model demonstrated the ability to reproduce global patterns of SIF observed by a satellite sensor and to capture the seasonality of SIF reasonably well over different regions (Qiu et al., 2019). The forcing data for BEPS-SIF simulations include relative humidity, wind speed, air temperature, surface atmosphere pressure, incoming solar shortwave flux, and total precipitation. At the three sites, LAI is obtained from the field measurements and used for SIF simulations for the SCOPE and BEPS models. The other main input parameters for the SCOPE and BEPS simulations are shown in Table S1 and Table S2.

Table S1 Main input parameters of three sites for the SCOPE simulations.

Parameter	Description	Unit	Shangqiu	Xilinhot	Jurong
C_{ab}	Leaf chlorophyll a+b content	μg/cm^2	80	20	60
Rdparam	Respiration	–	0.015	0.025	0.015
Slope (*m*)	Ball-Berry stomatal conductance parameter	–	9	4	9
$LIDF_a$	Leaf inclination parameter	–	-0.35	-1	-1
$LIDF_b$	Bimodality parameter	–	-0.15	0	0
V_{cmax}	Maximum carboxylation capacity	μmol/m^2	100	20	80
FQE	Fluorescence quantum yield efficiency	–	0.01	0.01	0.01

VZA	View zenith angle	Degree	0	0	0
RAA	Relative azimuth angle	Degree	0	0	0

Table S2 Main input parameters of three sites for the BEPS simulations.

Parameters	Description	Unit	Shangqiu	Xinlinhot	Jurong
V_{cmax}	Maximum carboxylation capacity	μmol/m^2/s	100	20	80
J_{cmax}	maximum electron transport rate	μmol/m^2/s	200	193	200
N	leaf nitrogen content	g/m^2	1.69	1.62	1.69
χ_n	slope of V_{cmax} variation with N	m^2/g	0.60	0.62	0.60
Slope (m)	slope in the Ball-Berry equation	–	9	4	9
Intercept (b)	intercept in the Ball-Berry equation	μmol/m^2/s	0.0011	0.0011	0.0011
Rdparam	Respiration	–	0.015	0.025	0.015
Ω	Clumping index	–	0.85	0.8	0.85

Appendix B.

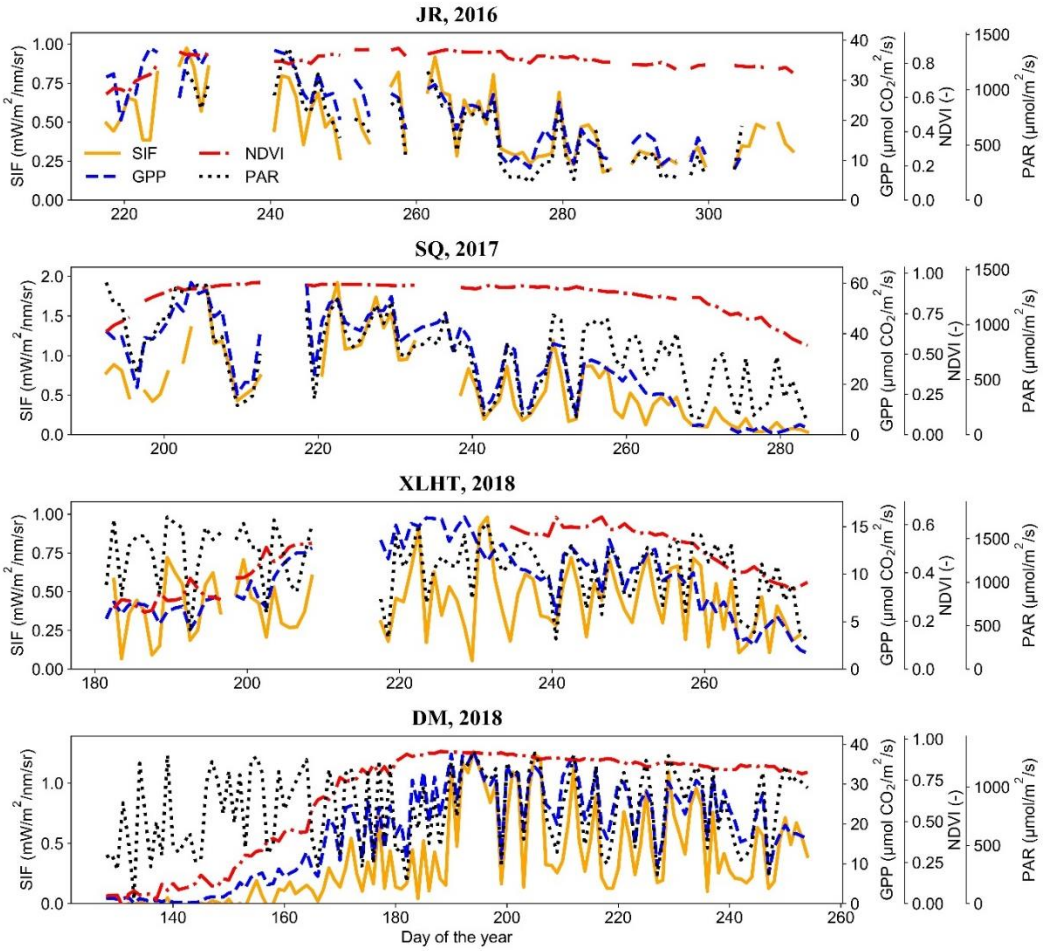

Figure S1. Seasonal variations of daily mean SIF, PAR, GPP and NDVI at four SIF sites. The names are identified in Table 1.

Appendix C. Calibration coefficients from different time

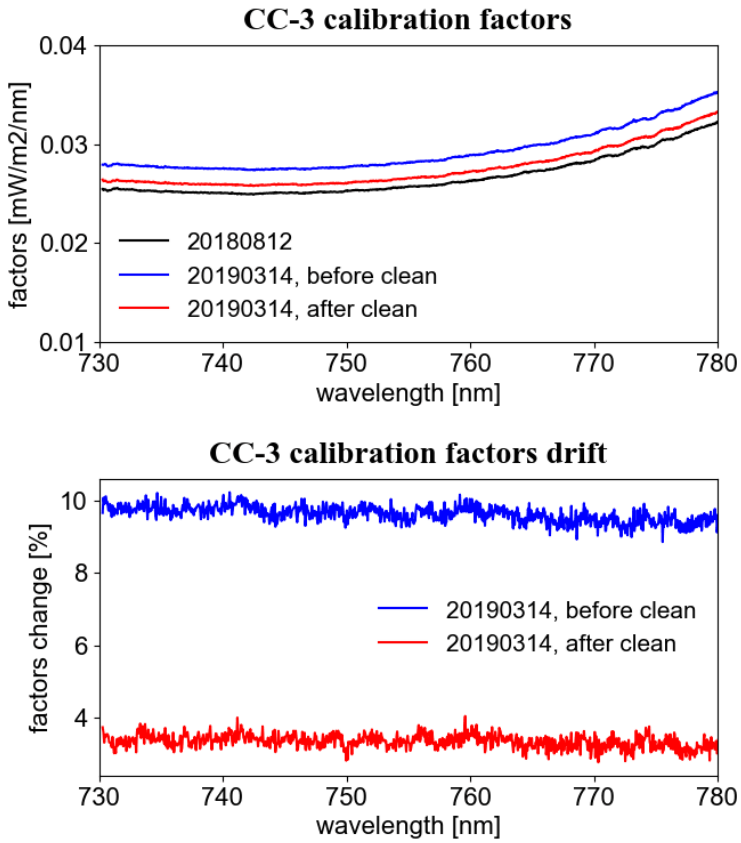

Figure S2. Three calibration coefficients acquired from two different times and before-after-cleaning dust, as well as fractions of change on the basis of coefficient obtained on August 12th 2018.

References

Aasen, H., Van Wittenberghe, S., Medina, N.S., Damm, A., Goulas, Y., Wieneke, S., Hueni, A., Malenovský, Z., Alonso, L., Pacheco-Labrador, J. Sun-induced chlorophyll fluorescence ii: Review of passive measurement setups, protocols, and their application at the leaf to canopy level. Remote Sens. 2019, 11, 927.

Alonso, L., Gómez-Chova, L., Vila-Francés, J., Amorós-López, J., Guanter, L., Calpe, J., et al. (2008). Improved Fraunhofer Line Discrimination method for vegetation fluorescence quantification. IEEE Geoscience and Remote Sensing Letters, 5(4), 620–624.

Baldocchi, D. (2008). Breathing of the terrestrial biosphere: lessons learned from a global network of carbon dioxide flux measurement systems. Aust. J. Bot., 56, 1–26,

Baldocchi, D. (2019). How eddy covariance flux measurements have contributed to our understanding of Global Change Biology. Global Change biology, 00, 1-19,

Balzarolo, M., Anderson, K., Nichol, C., Rossini, M., Vescovo, L.,Arriga, N., Wohlfahrt, G., Calvet, J.-C. C., Carrara, A., Cerasoli, S., Cogliati, S., Daumard, F., Eklundh, L., Elbers, J. A., Evrendilek, F., Handcock, R. N., Kaduk, J., Klumpp, K., Longdoz, B., Matteucci, G., Meroni, M., Montagnani, L., Ourcival, J.-M. M., Sánchez-Cañete, E. P., Pontailler, J.-Y. Y., Juszczak, R., Scholes, B., Martín, M. P., Pilar Martín, M., and Martín, M. P. (2011). Ground-based optical measurements at european flux sites: A review of methods, instruments and current controversies, Sensors, 11, 7954–7981.

Bendig, J., Gautam, D., Malenovský, Z., Lucieer, A. Influence of Cosine Corrector and UAS Platform Dynamics on Airborne Spectral Irradiance Measurements. In Proceedings of the 2018 IEEE International Geoscience and Remote Sensing Symposium (IGARSS), Valencia, Spain, 22–27 July 2018; pp. 8822–8825.

Cendrero-Mateo, M.P., Wieneke, S., Damm, A., Alonso, L., Pinto, F., Moreno, J., Guanter, L., Celesti, M., Rossini, M., Sabater, N., Cogliati, S., Julitta, T., Rascher, U., Goulas, Y., Aasen, H., Pacheco-Labrador, J., Mac Arthur, A. (2019). Sun-Induced Chlorophyll Fluorescence III: Benchmarking Retrieval Methods and Sensor Characteristics for Proximal Sensing. Remote Sensing, 11, 962.

Cogliati, S., Rossini, M., Julitta, T., Meroni, M., Schickling, A., Burkart, A., et al. (2015). Continuous and long-term measurements of reflectance and sun-induced chlorophyll fluorescence by using novel automated field spectroscopy systems. Remote Sensing of Environment, 164, 270-281.

Damm, A., Guanter, L., Paul-Limoges, E., van der Tol, C., Hueni, A., Buchmann, N., et al. (2015). Far-red sun-induced chlorophyll fluorescence shows ecosystem-specific relationships to gross primary production: An assessment based on observational and modeling approaches. Remote Sensing of Environment, 166, 91-105.

Drusch, M., Moreno, J., Del Bello, U., Franco, R., Goulas, Y., Huth, A., et al. (2017). The fluorescence explorer mission concept—ESA's Earth explorer 8. IEEE Transactions on Geoscience and Remote Sensing, 55, 1273-1284.

Du, S., Liu, L., Liu, X., Guo, J., Hu, J., Wang, S., & Zhang, Y.(2019). SIFSpec: Measuring Solar-Induced Chlorophyll Fluorescence Observations for Remote Sensing of Photosynthesis. Sensors, 19, 3009.

Du, S., Liu, L., Liu, X., Zhang, X., Zhang, X., Bi, Y., & Zhang, L. (2018) Retrieval of global terrestrial solar-induced chlorophyll fluorescence from TanSat satellite. Science Bulletin, 63, (22), 1502-1512.

Frankenberg, C., Fisher, J. B., Worden, J., Badgley, G., Saatchi, S. S., Lee, J. E., et al. (2011). New global observations of the terrestrial carbon cycle from GOSAT: Patterns of plant fluorescence with gross primary productivity. Geophysical Research Letters, 38, 351-365.

Frankenberg, C., Köhler, P., Magney, T.S., Geier, S., Lawson, P., Schwochert, M., et al. (2018). The Chlorophyll Fluorescence Imaging Spectrometer (CFIS), mapping far red fluorescence from aircraft. Remote Sensing of Environment, 217, 523-536.

Gamon, J. A., Coburn, C., Flanagan, L. B., Huemmrich, K. F., Kiddle,C., Sanchez-Azofeifa, G. A., et al. (2010). SpecNet revisited: bridging flux and remote sensing communities. Canadian Journal of Remote Sensing, 36, S376–S390.

Gamon, J. A., Rahman, A. F., Dungan, J. L., Schildhauer, M., & Huemmrich, K. F. (2006) Spectral Network (SpecNet) – what is it and why do we need it? Remote Sensing of Environment, 103, 227–235.

Gómez-Chova, L., Alonso, L., Amorós-López, J., Vila-Francés, J., del Valle-Tascón, S., Calpe, J., et al. (2006). Solar-induced fluorescence measurements using a field spectroradiometer. Earth observation for vegetation monitoring and water management. AIP Conference Proceedings, 852, 274–281.

Grossmann, K., Frankenberg, C., Magney, T. S., Hurlock, S. C., Seibt, U., & Stutz, J. (2018). PhotoSpec: A new instrument to measure spatially distributed red and far-red Solar-Induced Chlorophyll Fluorescence. Remote Sensing of Environment, 216, 311–327.

Gu, L., Wood, J. D., Chang, C. Y. Y., Sun, Y., & Riggs, J. S. (2019). Advancing Terrestrial Ecosystem Science With a Novel Automated Measurement System for Sun-Induced Chlorophyll Fluorescence for Integration With Eddy Covariance Flux Networks. Journal of Geophysical Research: Biogeosciences, 124(1), 127–146.

Guanter, L., Frankenberg, C., Dudhia, A., Lewis, P.E., Gómez-Dans, J., Kuze, A., et al. (2012). Retrieval and global assessment of terrestrial chlorophyll fluorescence from GOSAT space measurements. Remote Sensing of Environment, 121, 236-251.

Guanter, L., Zhang, Y., Jung, M., Joiner, J., Voigt, M., Berry, J.A., et al. (2014). Global and time-resolved monitoring of crop photosynthesis with chlorophyll fluorescence. Proceedings of the National Academy of Sciences of the United States of America, 111, E1327-E1333.

Hilker, T., Coops, N. C., Wulder, M. A., Black T. A., & Guy R. D. (2008). The use of remote sensing in light use efficiency based models of gross primary production: a review of current status and future requirements. Science of the Total Environment, 404, 411–423.

Huete, A. R., Didan, K., Miura, T., Rodriguez, E. P., Gao, X., & Ferreira, L. G. (2002), Overview of the radiometric and biophysical performance of the MODIS vegetation indices. Remote Sensing of Environment, 83, 195–213. https://doi.org/10.1016/S0034-4257(02)00096-2.

Joiner, J., Guanter, L., Lindstrot, R., Voigt, M., Vasilkov, A. P., Middleton, E. M., et al. (2013). Global monitoring of terrestrial chlorophyll fluorescence from moderate-spectral-resolution near-infrared satellite measurements: methodology, simulations, and application to GOME-2. Atmospheric Measurement Techniques, 6, 2803-2823.

Köhler, P., Frankenberg, C., Magney, T. S., Guanter, L., Joiner, J., & Landgraf, J. (2018). Global retrievals of Solar-Induced Chlorophyll Fluorescence with TROPOMI: First results and intersensor comparison to OCO-2. Geophysical Research Letters, 45, 10456-10463.

Köhler, P., Guanter L., Joiner J. (2015), A linear method for the retrieval of sun-induced chlorophyll fluorescence from GOME-2 and SCIAMACHY data, Atmospheric Measurement Techniques, 8(6), 2589-2608.

Lee, J. E., Berry, J. A., van der Tol, C., Yang, X., Guanter, L., Damm, A., et al. (2015). Simulations of chlorophyll fluorescence incorporated into the Community Land Model version 4. Global Change Biology, 21, 3469–3477.

Li, Z., Zhang, Q., Li, J., Yang, X., Wu, Y., Zhang, Z., et al. (2020). Solar-induced chlorophyll fluorescence and its link to canopy photosynthesis in maize from continuous ground measurements. Remote Sensing of Environment, 2020, 236, 111420.

Liu, X., Guo, J., Hu, J., Liu, L. Atmospheric Correction for Tower-Based Solar-Induced Chlorophyll Fluorescence Observations at O_2-A Band. Remote Sensing 2019, 11, (3).

Liu, X., Guanter, L., Liu, L.; Damm, A., Malenovský, Z., Rascher, U., Peng, D., Du, S., Gastellu-Etchegorry, J.-P. Downscaling of solar-induced chlorophyll fluorescence from canopy level to photosystem level using a random forest model. Remote Sens. Environ. 2018.

MacArthur, A.; Robinson, I.; Rossini, M.; Davis, N.; MacDonald, K. (2014). In A dual-field-of-view spectrometer system for reflectance and fluorescence measurements (piccolo doppio) and correction of etaloning, Proceedings of the Fifth International Workshop on Remote Sensing of Vegetation Fluorescence, pp 22-24.

Magney, T. S., Frankenberg, C., Köhler, P., North, G., Davis, T. S., Dold, C., et al. (2019). Disentangling Changes in the Spectral Shape of Chlorophyll Fluorescence: Implications for Remote Sensing of Photosynthesis. Journal of Geophysical Research: Biogeosciences. https://doi.org/10.1029/2019JG005029.

Maier, S. W., Günther, K. P., & Stellmes, M. (2003). Sun-induced fluorescence: A new tool for precision farming. In T. VanToai, D. Major, M. McDonald, J. Schepers, & L. Tarpley (Eds.), Digital imaging and spectral techniques: Applications to precision agriculture and crop physiology (pp. 209–222). Madison: American Society of Agronomy. https://doi.org/10.2134/asaspecpub66.c16.

Meroni, M., & Colombo, R. (2006). Leaf level detection of solar induced chlorophyll fluorescence by means of a subnanometer resolution spectroradiometer. Remote Sensing of Environment, 103, 438–448.

Meroni, M., Rossini, M., Guanter, L., Alonso, L., Rascher, U., Colombo, R., et al. (2009). Remote sensing of solar-induced chlorophyll fluorescence: review of methods and applications. Remote Sensing of Environment, 113(10), 2037-2051.

Mohammed, G.H., R. Colombo, E.M. Middleton, U. Rascher, C. van der Tol, L. Nedbal, Y. Goulas, O. Pérez-Priego, A. Damm, M. Meroni, J. Joiner, S. Cogliati, W. Verhoef, Z. Malenovský, J.P. Gastellu-Etchegorry, J.R. Miller, L. Guanter, J. Moreno, I. Moya, J.A. Berry, C. Frankenberg, P.J. Zarco-Tejada. (2019). Remote sensing of solar-induced chlorophyll fluorescence (SIF) in vegetation: 50 years of progress. Remote Sensing of Environment, 231, 10.1016/j.rse.2019.04.030

Moya, I., Ounis, A., Moise, N., & Goulas, Y. (2006). First airborne multiwavelenght passive chlorophyll fluorescence measurements over La Mancha (Spain) fields. In J. A. Sobrino (Ed.), Second recent advances in quantitative remote sensing (pp. 820–825). Spain: Publicacions de la Universitat de València. https://doi.org/10.13140/2.1.1031.9364.

Nichol, C.J., Drolet, G., Porcar-Castell, A., Wade, T., Sabater, N., Middleton, E.M., MacLellan, C., Levula, J., Mammarella, I., Vesala, T., Atherton, J. (2019). Diurnal and Seasonal Solar

994 Induced Chlorophyll Fluorescence and Photosynthesis in a Boreal Scots Pine Canopy. Remote
995 Sensing, 11, 273.

996 Moore, B., S. M. R. Crowell, P. .J. Rayner, J. Kumer, C. W. O'Dell, D. O'Brien, S. Utembe, I.
997 Polonsky, D. Schimel, J. Lemen. (2018). The Potential of the Geostationary Car- bon Cycle
998 Observatory (GeoCarb) to Provide Multi-scale Constraints on the Carbon Cycle in the Americas.
999 Frontiers in Environment Science, 6, 109, doi:10.3389/fenvs.2018.00109.

1000 Pacheco-Labrador, J., Hueni, A., Mihai, L., Sakowska, K., Julitta, T., Kuusk, J., Sporea, D.,
1001 Alonso, L., Burkart, A., Cendrero-Mateo, M.P., Aasen, H., Goulas, Y., Mac Arthur, A. (2019).
1002 Sun-Induced Chlorophyll Fluorescence I: Instrumental Considerations for Proximal
1003 Spectroradiometers. Remote Sensing, 11, 960.

1004 Pinto, F., Müller-Linow, M., Schickling, A., Cendrero-Mateo, M., Ballvora, A., Rascher, U.
1005 Multiangular Observation of Canopy Sun-Induced Chlorophyll Fluorescence by Combining
1006 Imaging Spectroscopy and Stereoscopy. Remote Sens. 2017, 9, 415.

1007 Porcar-Castell, A., Mac Arthur, A., Rossini, M., Eklundh, L., Pacheco-Labrador, J., Anderson,
1008 K., et al. (2015). EUROSPEC: at the interface between remote-sensing and ecosystem CO_2 flux
1009 measurements in Europe. Biogeosciences, 12(20):6103-6124. https://doi.org/10.5194/bg-12-
1010 6103-2015.

1011 Qiu, B., Chen, J. M., Ju, W., Zhang, Q., Zhang, Y. (2019). Simulating emission and scattering of
1012 solar-induced chlorophyll fluorescence at far-red band in global vegetation with different canopy
1013 structures. Remote Sensing of Environment, 233, 111373.
1014 https://doi.org/10.1016/j.rse.2019.111373.

1015 Quan, Q., Tian, D., Luo, Y., Zhang, F., Crowther. T. W., Zhu, K., et al. (2019). Water scaling of
1016 ecosystem carbon cycle feedback to climate warming. Science Advances, 5(8): evva1131.
1017 https://doi.org/10.1126/sciadv.aav1131.

1018 Raczka, B., Porcar-Castell, A., Magney, T., Lee, J. E., Köhler, P., Frankenberg, C., et al. (2018).
1019 Sustained Non-Photochemical Quenching Shapes the Seasonal Pattern of Solar-Induced
1020 Fluorescence at a High-Elevation Evergreen Forest. Journal of Geophysical Research:
1021 Biogeosciences, 124(7), 2005-2020.

1022 Rascher U., Alonso L., Burkart A., Cilia C., Cogliati S., Colombo R., Damm A., Drusch M.,
1023 Guanter L., Hanus J., Hyvrinen T., Julitta T., Jussila J., Kataja K., Kokkalis P., Kraft S., Kraska
1024 T., Matveeva M., Moreno J., Muller O., Panigada C., Pikl M., Pinto F., Prey L., Pude R., Rossini
1025 M., Schickling A., Schurr U., Schttemeyer D., Verrelst J., Zemek F. Sun-induced fluorescence a
1026 new probe of photosynthesis: first maps from the imaging spectrometer HyPlant. Global Change
1027 Biology, 21 (2015), 4673-4684.

1028 Sabater, N., Vicent, J., Alonso, L., Verrelst, J., Middleton, E.M., Porcar-Castell, A., Moreno, J.
1029 Compensation of Oxygen transmittance effects for proximal sensing retrieval of canopy–leaving
1030 sun–induced chlorophyll fluorescence. Remote Sensing, 2018, 10, 1551.

1031 Shan, N., Ju, W. M., Migliavacca, M., Martini, D., Guanter, L., Chen, J. M., et al. (2019),
1032 Modeling canopy conductance and transpiration from solar-induced chlorophyll fluorescence,
1033 Agricultural and Forestry Meteorology, 268, 189-201.

1034 Sun, Y., Frankenberg, C., Jung, M., Joiner, J., Guanter, L., Köhler, P., & Magney, T. (2018).
1035 Overview of Solar-Induced chlorophyll Fluorescence (SIF) from the Orbiting Carbon

Observatory-2: Retrieval, cross-mission comparison, and global monitoring for GPP. Remote Sensing of Environment, 209, 808-823.

Theisen, A. F. (2002). Detecting chlorophyll fluorescence from orbit: The Fraunhofer Line Depth model. In R. S. Muttiah (Ed.), From Laboratory Spectroscopy to Remotely Sensed Spectra of Terrestrial Ecosystems (pp. 203–232). Dordrecht: Kluwer Academic Publishers1-4020-0753-1. https://doi.org/10.1007/978-94-017-1620-8_10.

Tong, X., Mu, Y., Zhang, J., Meng, P., &Li, J., (2019). Water stress controls on carbon flux and water use efficiency in a warm-temperate mixed plantation. Journal of Hydrology, 571, 669-678.

Van der Tol, C., Verhoef, W., Timmermans, J., Verhoef, A., & Su, Z. (2009). An integrated model of soil-canopy spectral radiances, photosynthesis, fluorescence, temperature and energy balance. Biogeosciences, 6, 3109-3129.

Wang, H., Han, D., Mu, Y., Jiang, L., Yao, X., Bai, Y., et al. (2019). Landscape-level vegetation classification and fractional woody and herbaceous vegetation cover estimation over the dryland ecosystems by unmanned aerial vehicle platform. Agricultural and Forest Meteorology, 278, 107665. https://doi.org/10.1016/j.agrformet.2019.107665.

Wieneke, S., Burkart, A., Cendrero-Mateo, M. P., Julitta, T., Rossini, M., & Schickling, A., et al. (2018). Linking photosynthesis and sun-induced fluorescence at sub-daily to seasonal scales. Remote Sensing of Environment, 219, 247-258.

Wang, C., Yu, G., Zhou, G., Yan, J., Zhang, L., Wang, X., et al. (2006). CO2 flux evaluation over the evergreen coniferous and broad-leaved mixed forest in Dinghushan, china. Science in China, 49(2 Supplement), 127-138.

Yang, P., Luo, J., Yuan, D., & He, Q. (2009). Response of spring water hydrochemical behaviors to rainfall in karst subterranean river system. Journal of Hydraulic Engineering, 40(1): 67-74.

Yang, P., & van der Tol, C. (2018). Linking canopy scattering of far-red sun-induced chlorophyll fluorescence with reflectance. Remote Sensing of Environment, 209, 456-467.

Yang, K., Ryu, Y., Dechant, B., Berry, J.A., Hwang, Y., Jiang, C., et al. (2018a). Sun-induced chlorophyll fluorescence is more strongly related to absorbed light than to photosynthesis at half-hourly resolution in a rice paddy. Remote Sensing of Environment, 216, 658-673.

Yang, X., Shi, H., Stovall, A., Guan, K., Miao, G., Zhang, Y., et al. (2018b). FluoSpec 2-An automated field spectroscopy system to monitor canopy solar-induced fluorescence. Sensors, 18, 2063. https://doi.org/10.3390/s18072063.

Yang, X., Tang, J., Mustard, J. F., Lee, J.-E., Rossini, M., Joiner, J., et al. (2015). Solar-induced chlorophyll fluorescence that correlates with canopy photosynthesis on diurnal and seasonal scales in a temperate deciduous forest. Geophysical Research Letters, 42, 2977-2987.

Yu, G.R., Wen, X.F., Sun, X. M., Tanner, B.D., Li, X., & Chen, J.Y. (2006). Overview of ChinaFLUX and evaluation of its eddy covariance measurement. Agricultural and Forest Meteorology, 137, 125-137.

Yu, G.R., Zhang, L.M., Su, X. M., (2010). Progresses and prospects of Chinese terrestrial ecosystem flux observation and research network (ChinaFLUX). Progress in Geography, 33(7), 903-917.

Zhang, Q., Zhang, X., Li, Z., Wu, Y., & Zhang, Y. (2019). Comparison of Bi-Hemispherical and Hemispherical-Conical Configurations for In Situ Measurements of Solar-Induced Chlorophyll Fluorescence. Remote Sensing, 11, 2642. https://doi.org/10.3390/rs11222642.

Zhang, B., Li, S., Chen, S., Ren, T., Yang, Z., Zhao, H., et al. (2016). Arbuscular mycorrhizal fungi regulate soil respiration and its response to precipitation change in a semiarid steppe. Scientific Report, 6, 19990. https://doi.org/10.1038/srep19990.

Zeng, Y., Badgley, G., Dechant, B., Ryu, Y., Chen, M., & Berry, J. (2019b). A practical approach for estimating the escape ratio of near-infrared solar-induced chlorophyll fluorescence. Remote Sensing of Environment, 211209.

Zhang, Z.Y., Chen, J.M., Guanter, L., He, L.M., & Zhang, Y.G. (2019). From canopy-leaving to total canopy far-red fluorescence emission for remote sensing of photosynthesis: first results from TROPOMI. Geophysical Research Letters, 46, 12030-12040.

Zhang, Z., Zhang, Y., Zhang, Q., Chen, Jing M., Porcar-Castell, A., Guanter, L., Wu, Y., Zhang, X., Wang, Z., Ding, D., Li, Z. Assessing bi-directional effects on the diurnal cycle of measured solar-induced chlorophyll fluorescence in crop canopies. Agricultural and Forest Meteorology, 2020, https://doi.org/10.1016/j.agrformet.2020.108147.

Zhu, J., Zhang Y., Yang, X., Chen, N., Li, S., Wang, P., Jiang, L. (2020). Warming alters plant phylogenetic and functional community structure. Journal of Ecology, 2020, DOI:10.1111/1365-2745.13448

Figure 1.

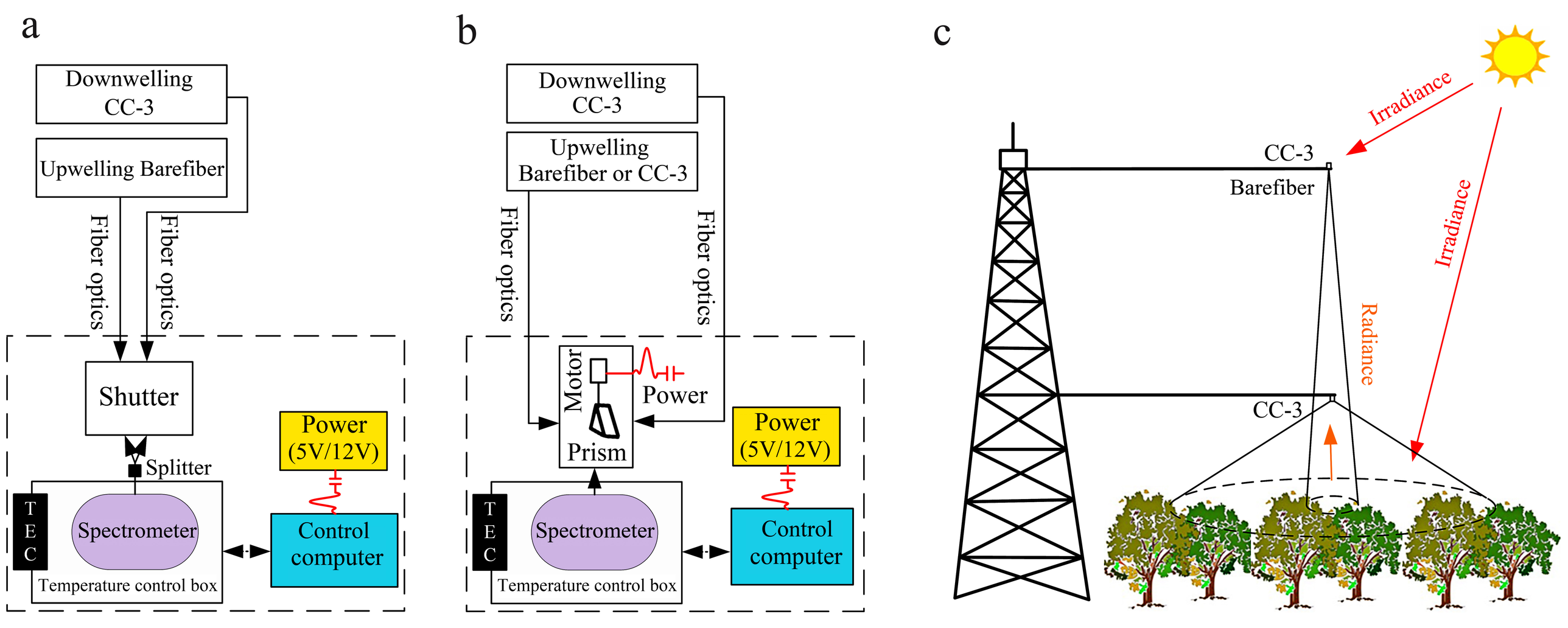
a
Downwelling CC-3
Upwelling Barefiber
Fiber optics
Fiber optics
Shutter
Splitter
Power (5V/12V)
T E C
Spectrometer
Control computer
Temperature control box
b
Downwelling CC-3
Upwelling Barefiber or CC-3
Fiber optics
Fiber optics
Motor
Power
Prism
Power (5V/12V)
T E C
Spectrometer
Control computer
Temperature control box
c
Irradiance
CC-3
Barefiber
Irradiance
Radiance
CC-3

Figure 2.

DHS

BB

DHS

HY

XTS

HL

DM

QYZ

QYZ

SHQ

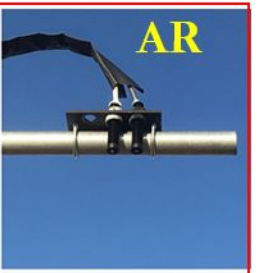
AR

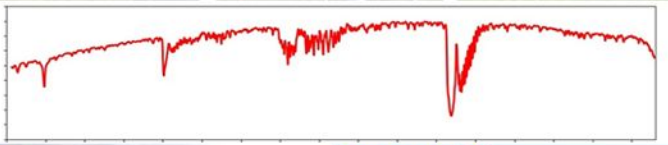

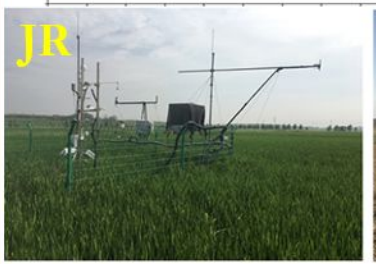
JR

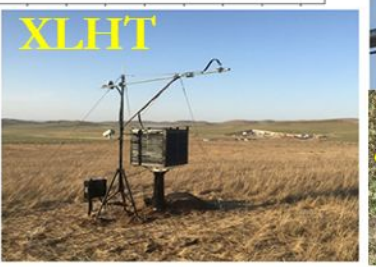
XLHT

XLHT

JDS

Figure 3.

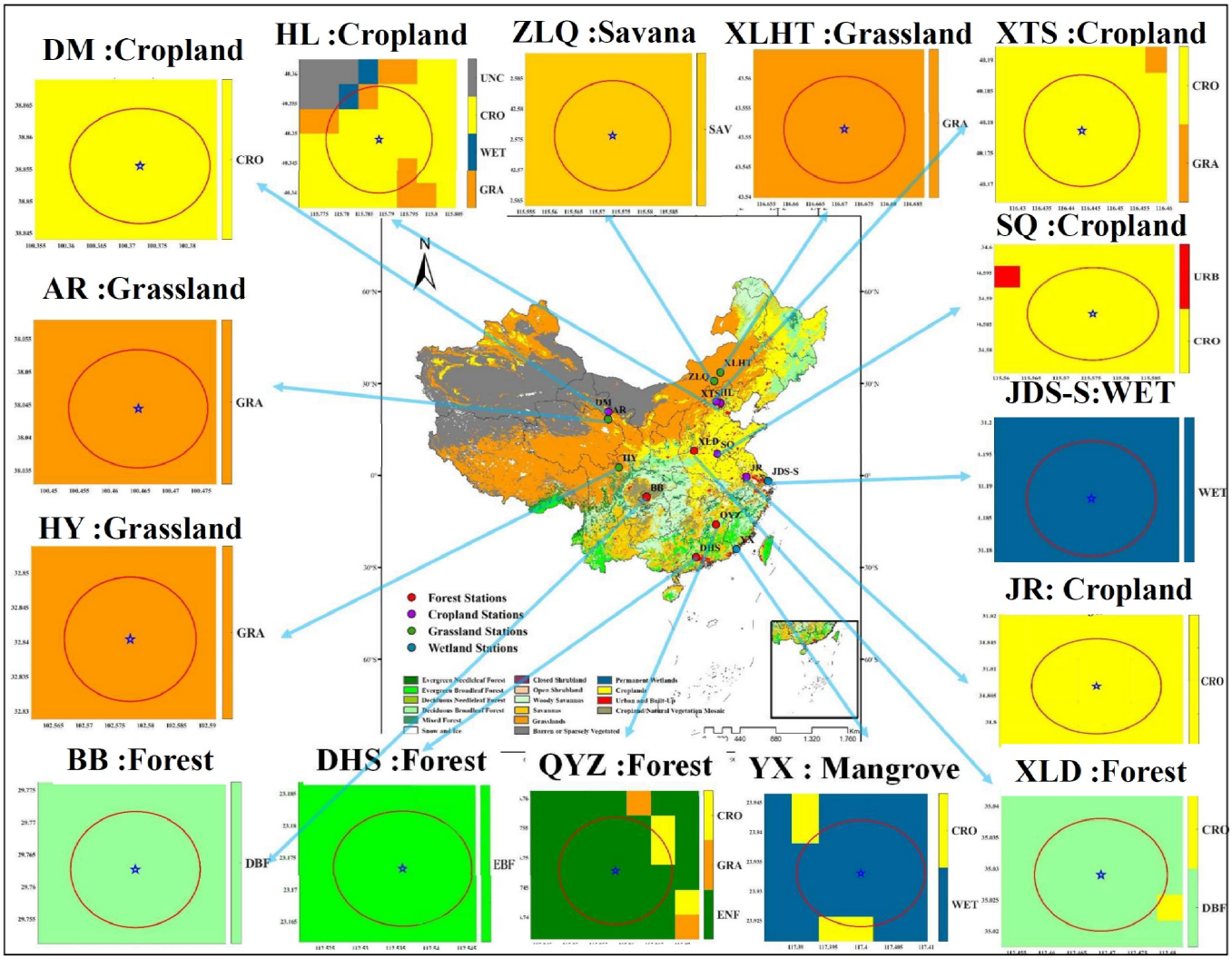
DM :Cropland
CRO
HL :Cropland
UNC
CRO
WET
GRA
ZLQ :Savana
SAV
XLHT :Grassland
GRA
XTS :Cropland
CRO
GRA
SQ :Cropland
URB
CRO
AR :Grassland
GRA
JDS-S:WET
WET
HY :Grassland
GRA
JR: Cropland
CRO
BB :Forest
DBF
DHS :Forest
EBF
QYZ :Forest
CRO
GRA
ENF
YX : Mangrove
CRO
WET
XLD :Forest
CRO
DBF
N
DM
AR
HL
ZLQ
XLHT
XTS
SQ
XLD
JR
JDS-S
HY
BB
QYZ
DHS
YX
Forest Stations
Cropland Stations
Grassland Stations
Wetland Stations

Figure 4.

Research Advances

More

- 叶绿素荧光遥感观测网络进展
  2019-02-19

News

More

- ChinaSpec网站在进行最后系统测试
  2019-11-17
- 网站仍在测试阶段
  2019-06-04

Visit Record

Site Query

Input Site Name Search

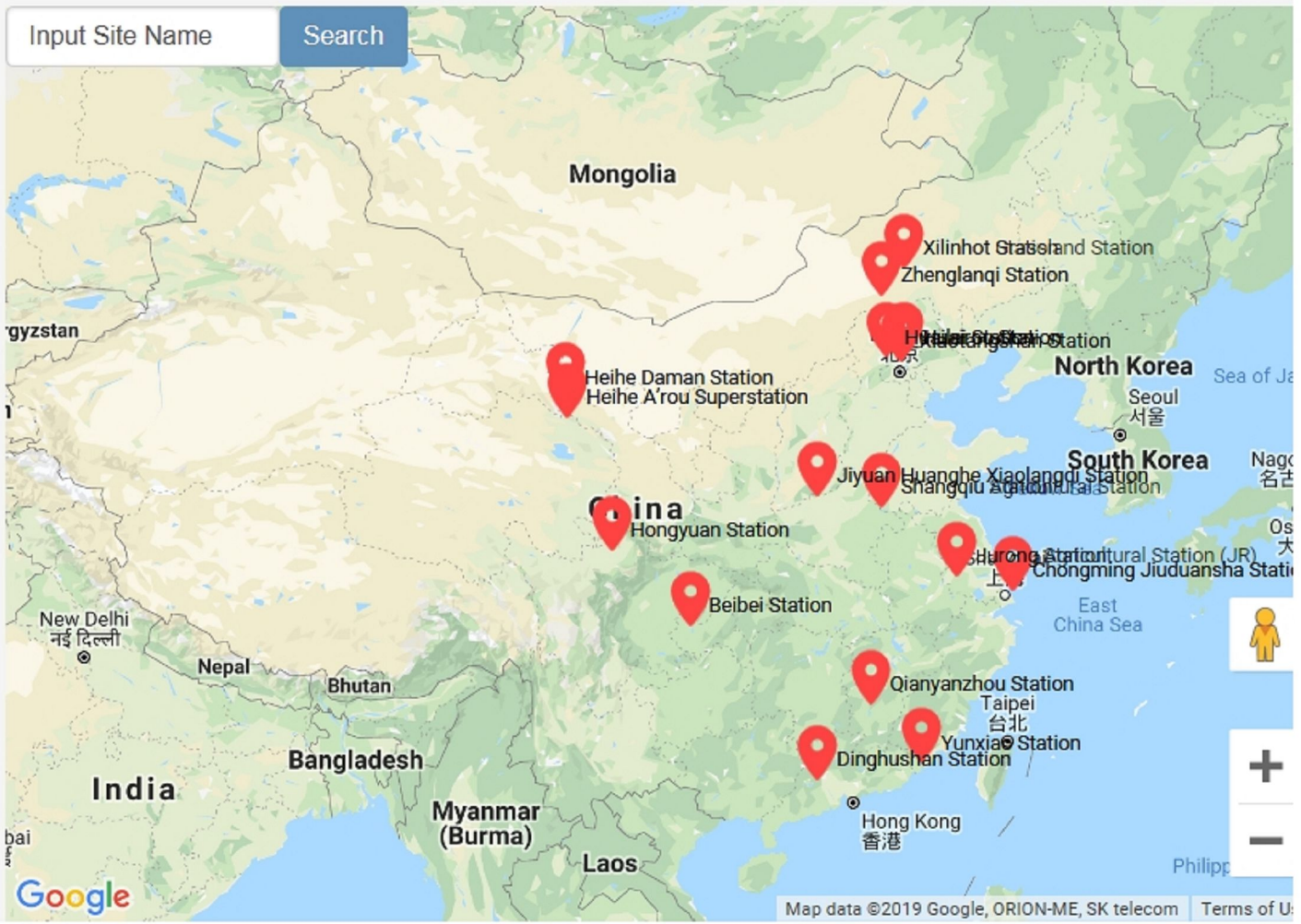

Figure 5.

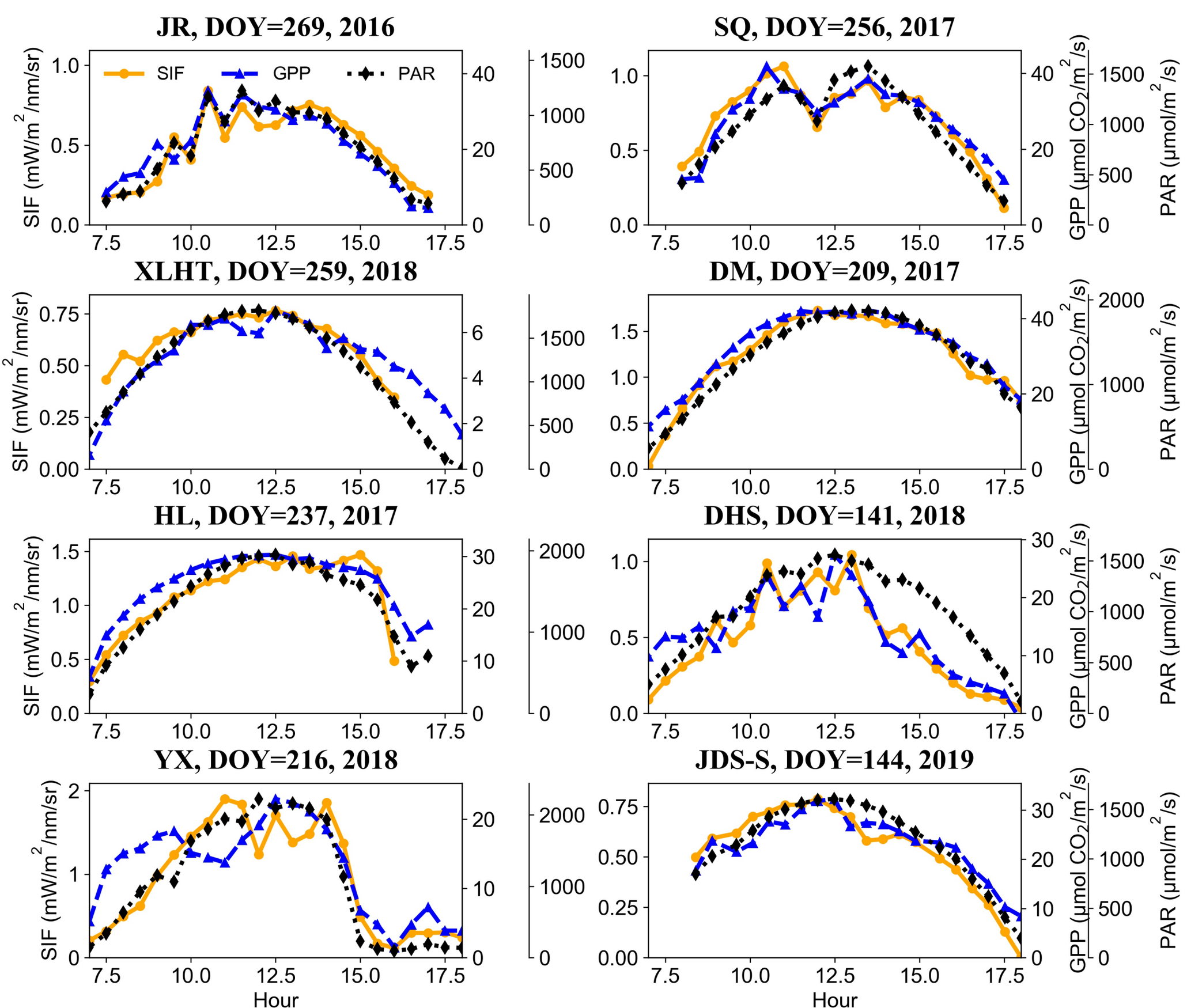
JR, DOY=269, 2016
SQ, DOY=256, 2017
XLHT, DOY=259, 2018
DM, DOY=209, 2017
HL, DOY=237, 2017
DHS, DOY=141, 2018
YX, DOY=216, 2018
JDS-S, DOY=144, 2019
SIF
GPP
PAR
SIF (mW/m2/nm/sr)
GPP (μmol CO2/m2/s)
PAR (μmol/m2/s)
Hour

Figure 6.

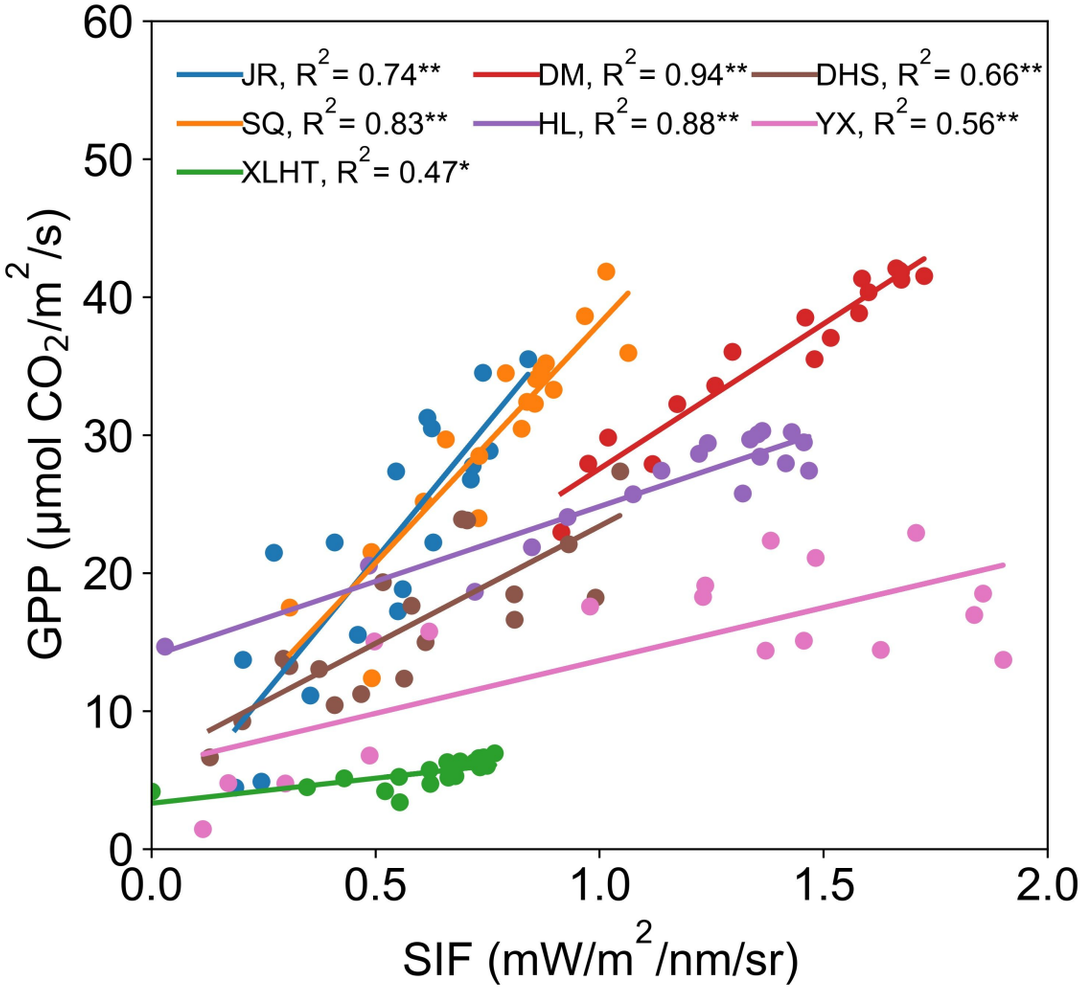
JR, R2= 0.74**
DM, R2= 0.94**
DHS, R2= 0.66**
SQ, R2= 0.83**
HL, R2= 0.88**
YX, R2= 0.56**
XLHT, R2= 0.47*
GPP (μmol CO2/m2/s)
SIF (mW/m2/nm/sr)
0
10
20
30
40
50
60
0.0
0.5
1.0
1.5
2.0

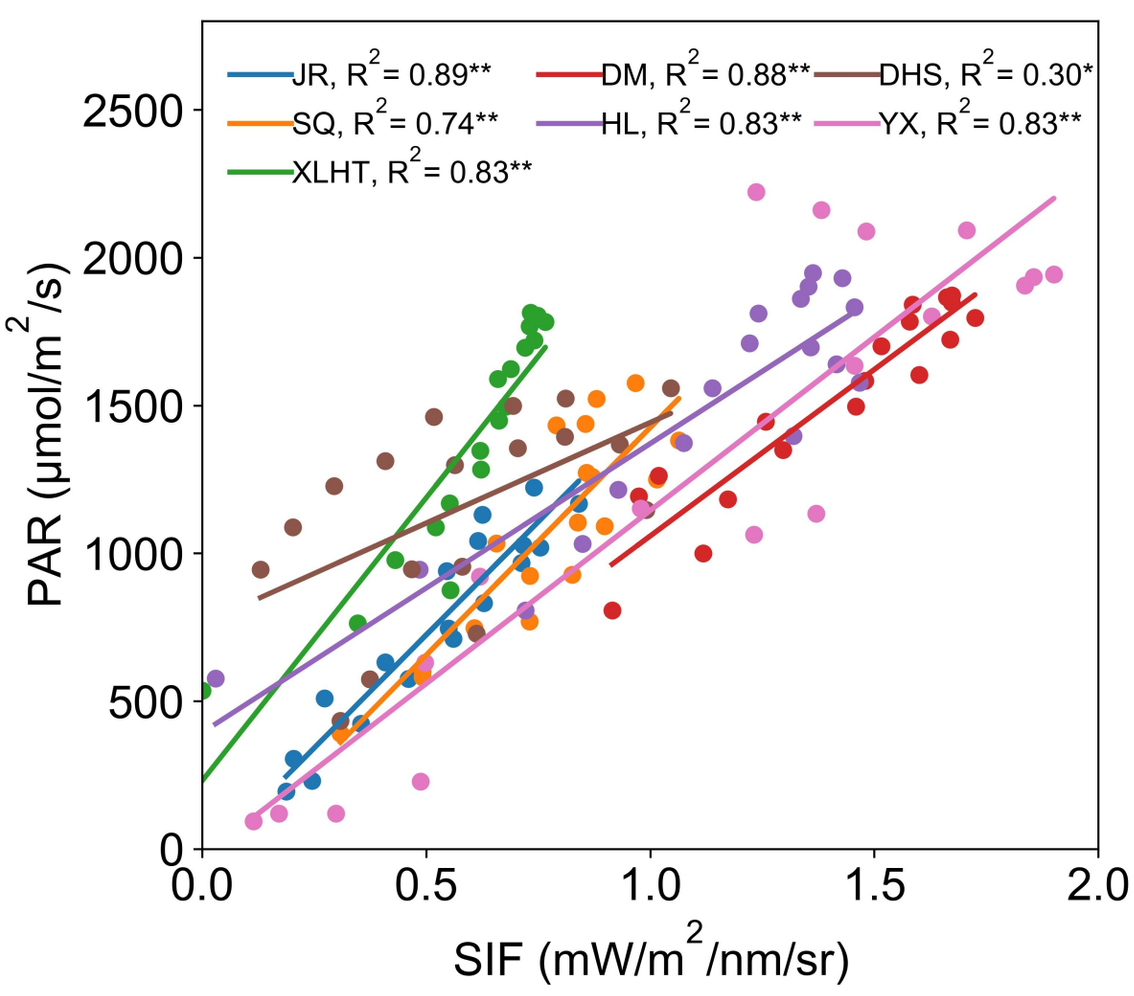
JR, R2= 0.89**
DM, R2= 0.88**
DHS, R2= 0.30*
SQ, R2= 0.74**
HL, R2= 0.83**
YX, R2= 0.83**
XLHT, R2= 0.83**
PAR (μmol/m2/s)
SIF (mW/m2/nm/sr)
0
500
1000
1500
2000
2500
0.0
0.5
1.0
1.5
2.0

Figure 6.

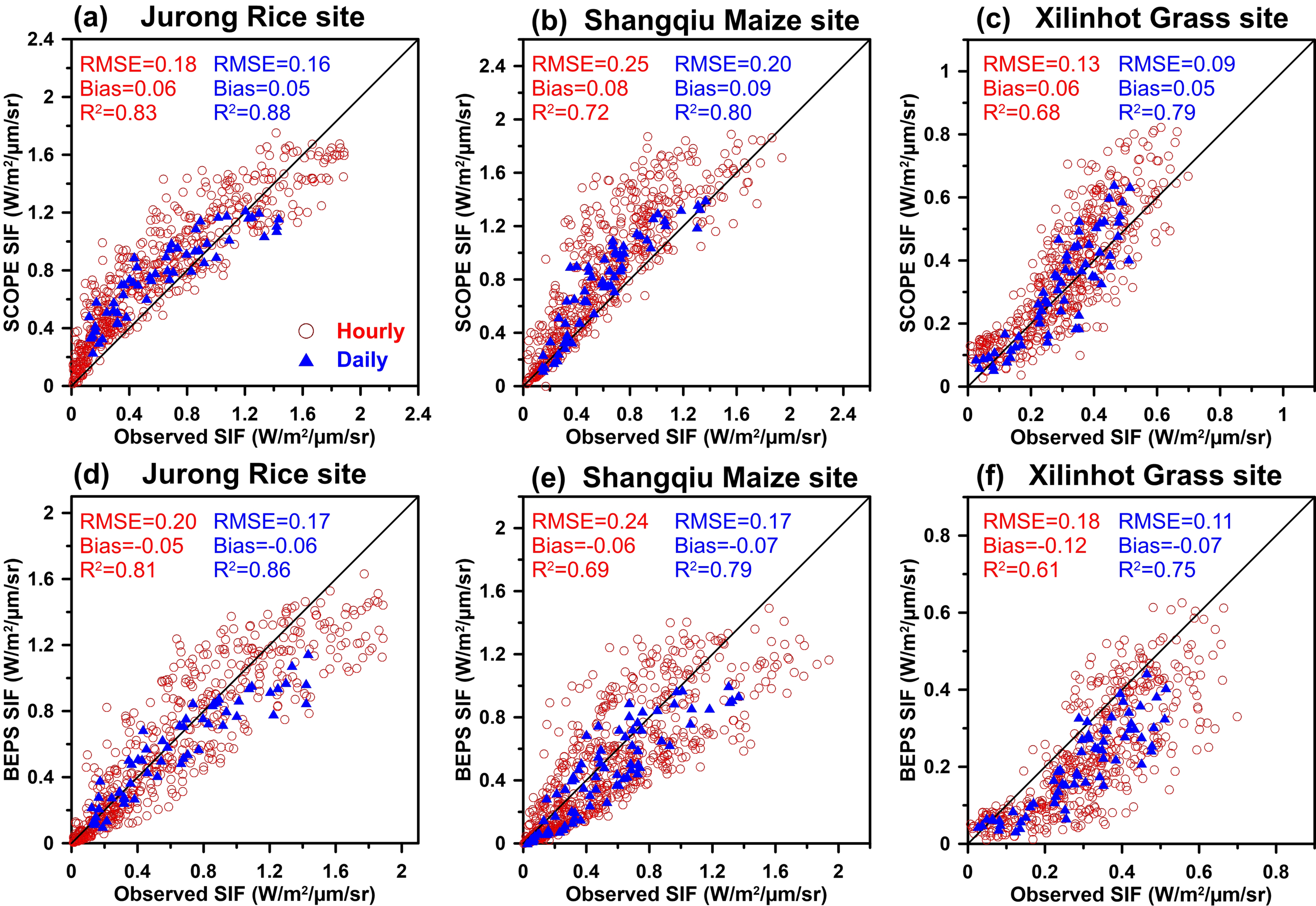
(a) Jurong Rice site
RMSE=0.18
Bias=0.06
R²=0.83
RMSE=0.16
Bias=0.05
R²=0.88
Hourly
Daily
SCOPE SIF (W/m²/μm/sr)
Observed SIF (W/m²/μm/sr)
(b) Shangqiu Maize site
RMSE=0.25
Bias=0.08
R²=0.72
RMSE=0.20
Bias=0.09
R²=0.80
SCOPE SIF (W/m²/μm/sr)
Observed SIF (W/m²/μm/sr)
(c) Xilinhot Grass site
RMSE=0.13
Bias=0.06
R²=0.68
RMSE=0.09
Bias=0.05
R²=0.79
SCOPE SIF (W/m²/μm/sr)
Observed SIF (W/m²/μm/sr)
(d) Jurong Rice site
RMSE=0.20
Bias=-0.05
R²=0.81
RMSE=0.17
Bias=-0.06
R²=0.86
BEPS SIF (W/m²/μm/sr)
Observed SIF (W/m²/μm/sr)
(e) Shangqiu Maize site
RMSE=0.24
Bias=-0.06
R²=0.69
RMSE=0.17
Bias=-0.07
R²=0.79
BEPS SIF (W/m²/μm/sr)
Observed SIF (W/m²/μm/sr)
(f) Xilinhot Grass site
RMSE=0.18
Bias=-0.12
R²=0.61
RMSE=0.11
Bias=-0.07
R²=0.75
BEPS SIF (W/m²/μm/sr)
Observed SIF (W/m²/μm/sr)

Figure 8.

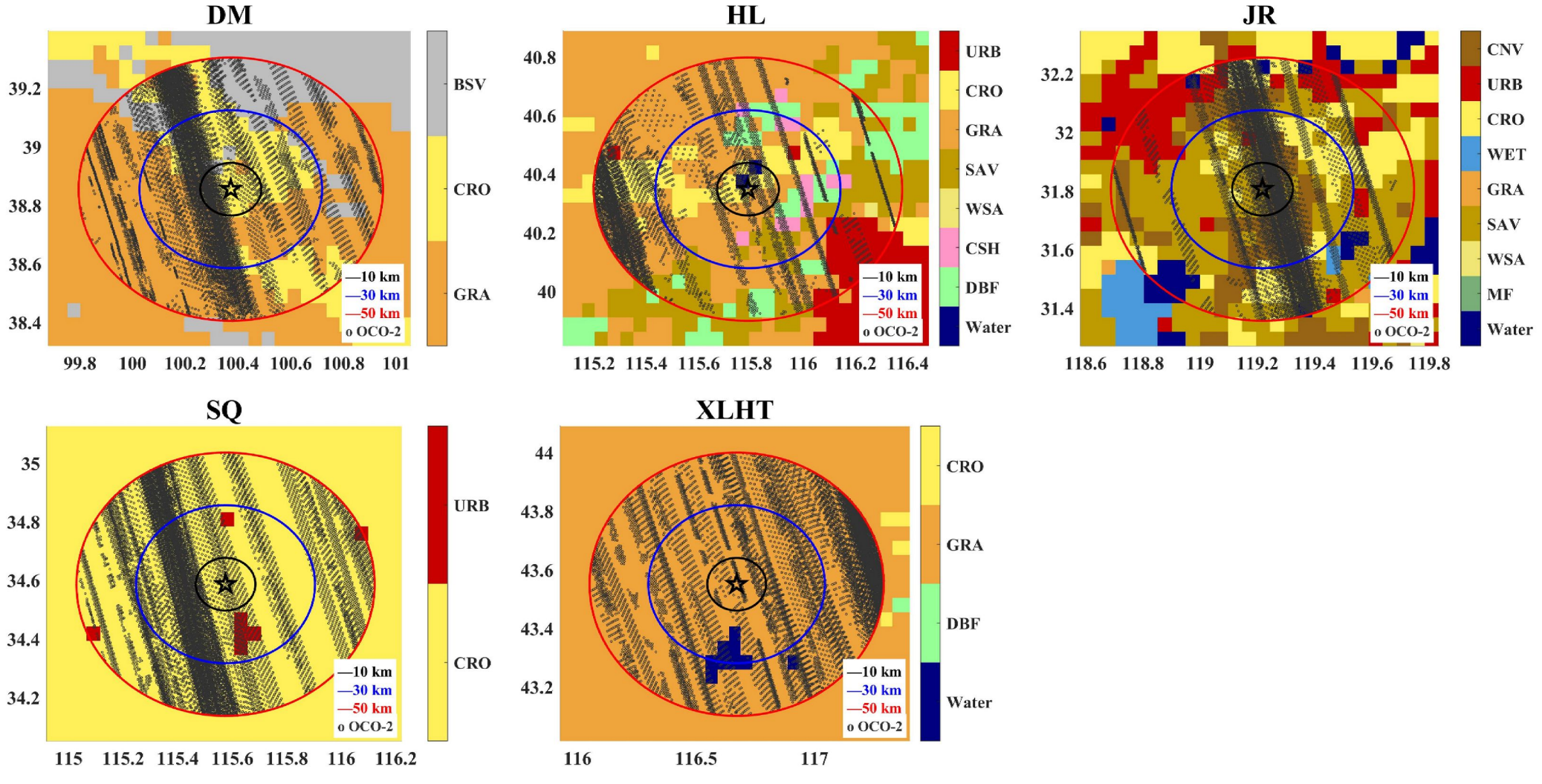
DM
39.2
39
38.8
38.6
38.4
99.8
100
100.2
100.4
100.6
100.8
101
BSV
CRO
GRA
—10 km
—30 km
—50 km
o OCO-2
HL
40.8
40.6
40.4
40.2
40
115.2
115.4
115.6
115.8
116
116.2
116.4
URB
CRO
GRA
SAV
WSA
CSH
DBF
Water
—10 km
—30 km
—50 km
o OCO-2
JR
32.2
32
31.8
31.6
31.4
118.6
118.8
119
119.2
119.4
119.6
119.8
CNV
URB
CRO
WET
GRA
SAV
WSA
MF
Water
—10 km
—30 km
—50 km
o OCO-2
SQ
35
34.8
34.6
34.4
34.2
115
115.2
115.4
115.6
115.8
116
116.2
URB
CRO
—10 km
—30 km
—50 km
o OCO-2
XLHT
44
43.8
43.6
43.4
43.2
116
116.5
117
CRO
GRA
DBF
Water
—10 km
—30 km
—50 km
o OCO-2

Figure 9.

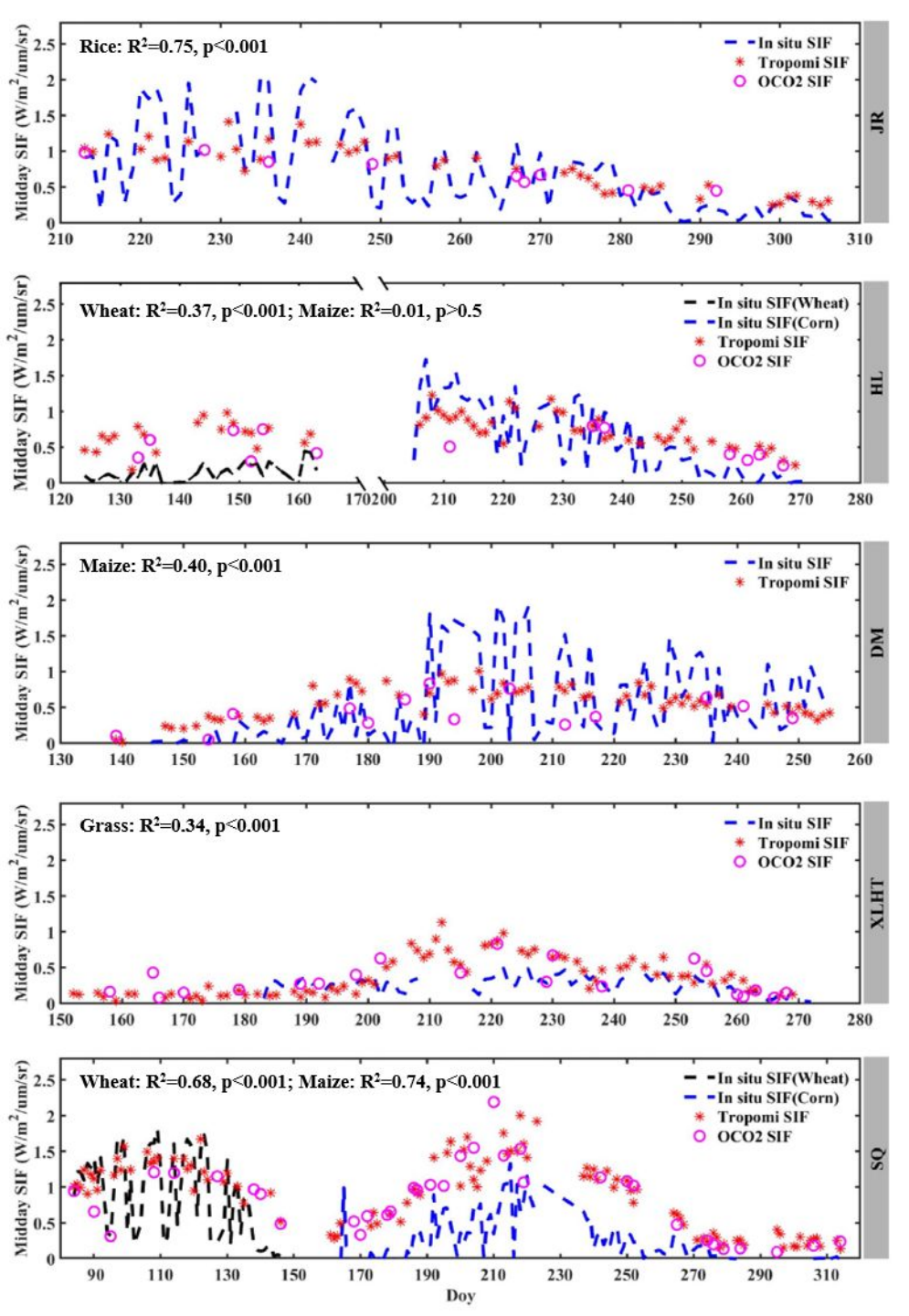
Rice: R²=0.75, p<0.001
In situ SIF
Tropomi SIF
OCO2 SIF
JR
Midday SIF (W/m²/um/sr)
Wheat: R²=0.37, p<0.001; Maize: R²=0.01, p>0.5
In situ SIF(Wheat)
In situ SIF(Corn)
HL
Maize: R²=0.40, p<0.001
DM
Grass: R²=0.34, p<0.001
XLHT
Wheat: R²=0.68, p<0.001; Maize: R²=0.74, p<0.001
SQ
Doy